Protostars as cosmic-ray factories

Marco Padovani

INAF-Osservatorio Astrofisico di Arcetri - Firenze

Patrick Hennebelle – Alexandre Marcowith – Katia Ferrière
Daniele Galli – Al Glassgold

Padovani, M., Hennebelle, P., Marcowith, A. & Ferrière, K. (2015) A&A 582, L13
Padovani, M., Marcowith, A., Hennebelle, P. & Ferrière, K. (2016) A&A 590, A8
Padovani, M., Marcowith, A., Hennebelle, P. & Ferrière, K. (2017) PPCF, 59, 014002

Cosmic rays and interstellar medium in one slide

CRs

astrochemistry

see e.g. Caselli & Ceccarelli (2012) for a recent review

collapse timescale

Nakano+ (2002)
Padovani+ (2013,2014)

gas temperature

Glassgold & Langer (1973)
Cravens & Dalgarno (1978)
Dalgarno+ (1999)
Glassgold+ (2012)
Galli & Padovani (2015)

dust grain charge

Prasad & Tarafdar (1983)
Cecchi-Pestellini & Aiello (1992)
Shen+ (2004)
Ivlev+ (2015)

(production of light elements, γ-ray emission through π^0 decay...)

Cosmic rays and ASTROCHEMISTRY

see Caselli & Ceccarelli (2012) for a recent review

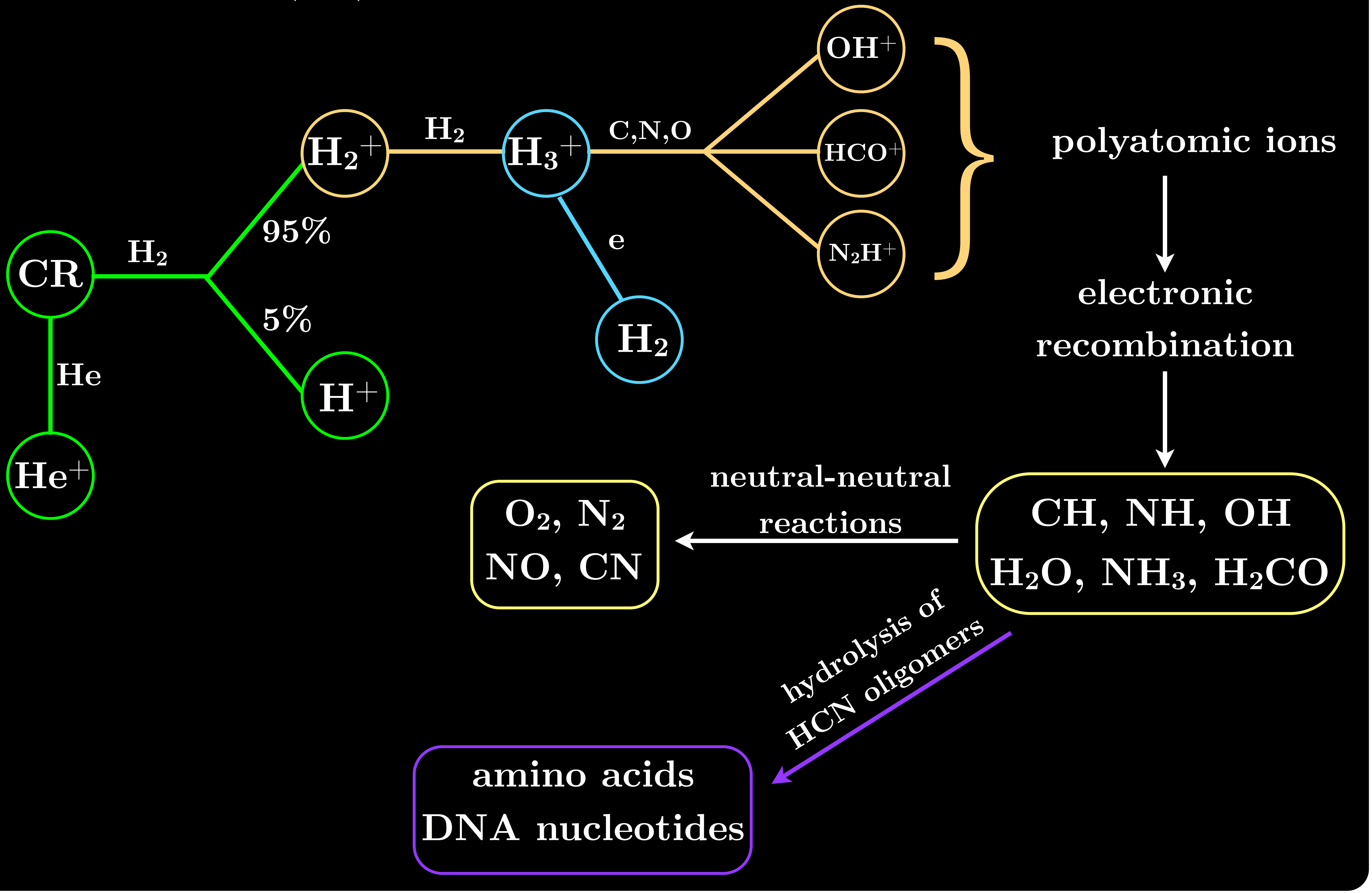

CR

H_2

95%

H_2^+

H_2

H_3^+

C,N,O

OH^+

HCO^+

N_2H^+

e

H_2

5%

H^+

He

He^+

polyatomic ions

electronic recombination

CH, NH, OH

H_2O, NH_3, H_2CO

neutral-neutral reactions

O_2, N_2

NO, CN

hydrolysis of HCN oligomers

amino acids

DNA nucleotides

Cosmic-ray ionisation rate

(number of ionisation per second)

ζ [s^{-1}] → *key-brick parameter:*

— chemical models (interpretation of observed abundances);

— non-ideal MHD simulations (study of the collapse of a molecular cloud core and the formation of a protostellar disc);

$$\zeta = 4\pi \int j(E)\sigma(E)\mathrm{d}E$$

Cosmic-ray ionisation rate

CR protons

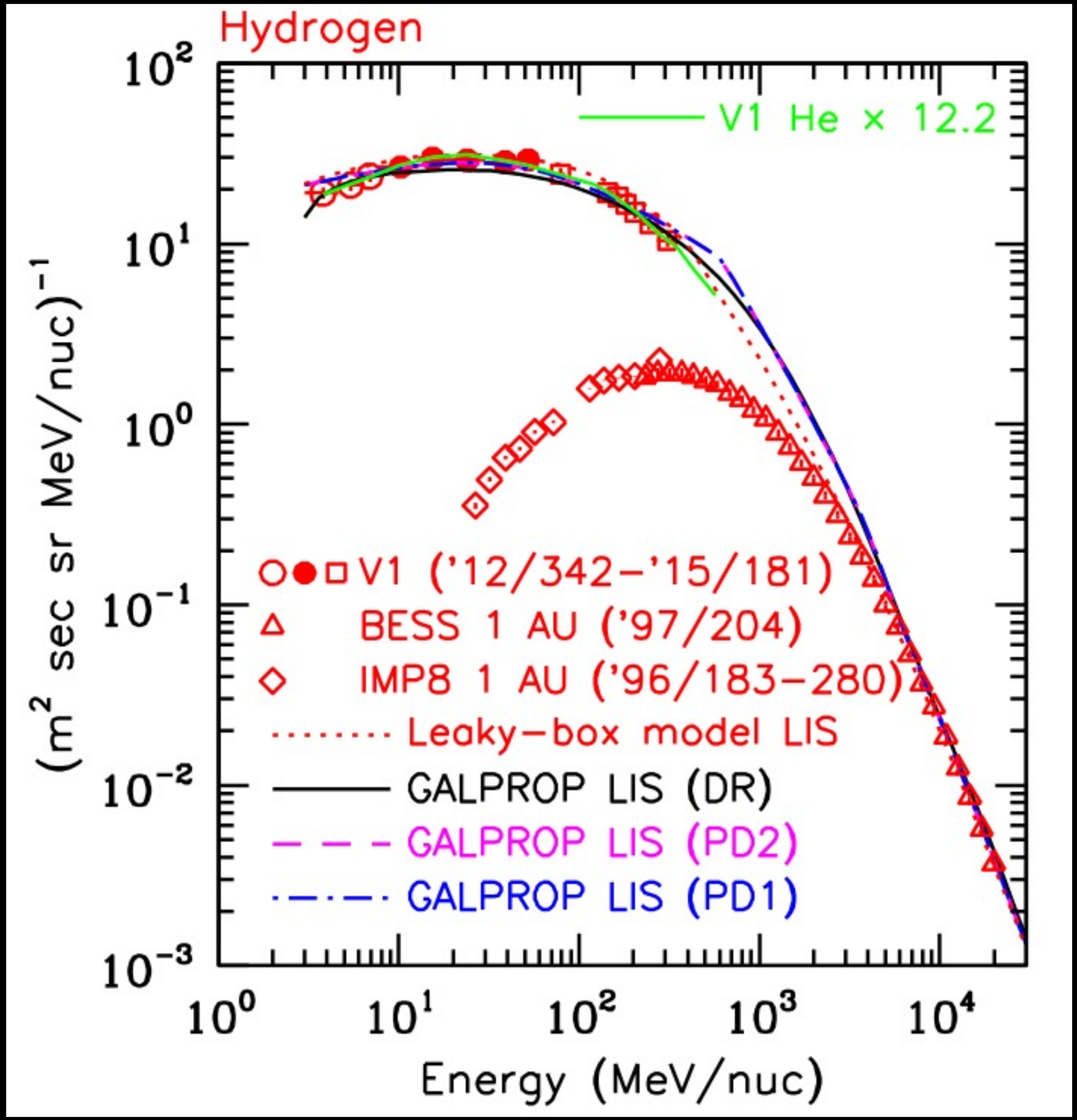

Cummings+ (2016)

CR electrons

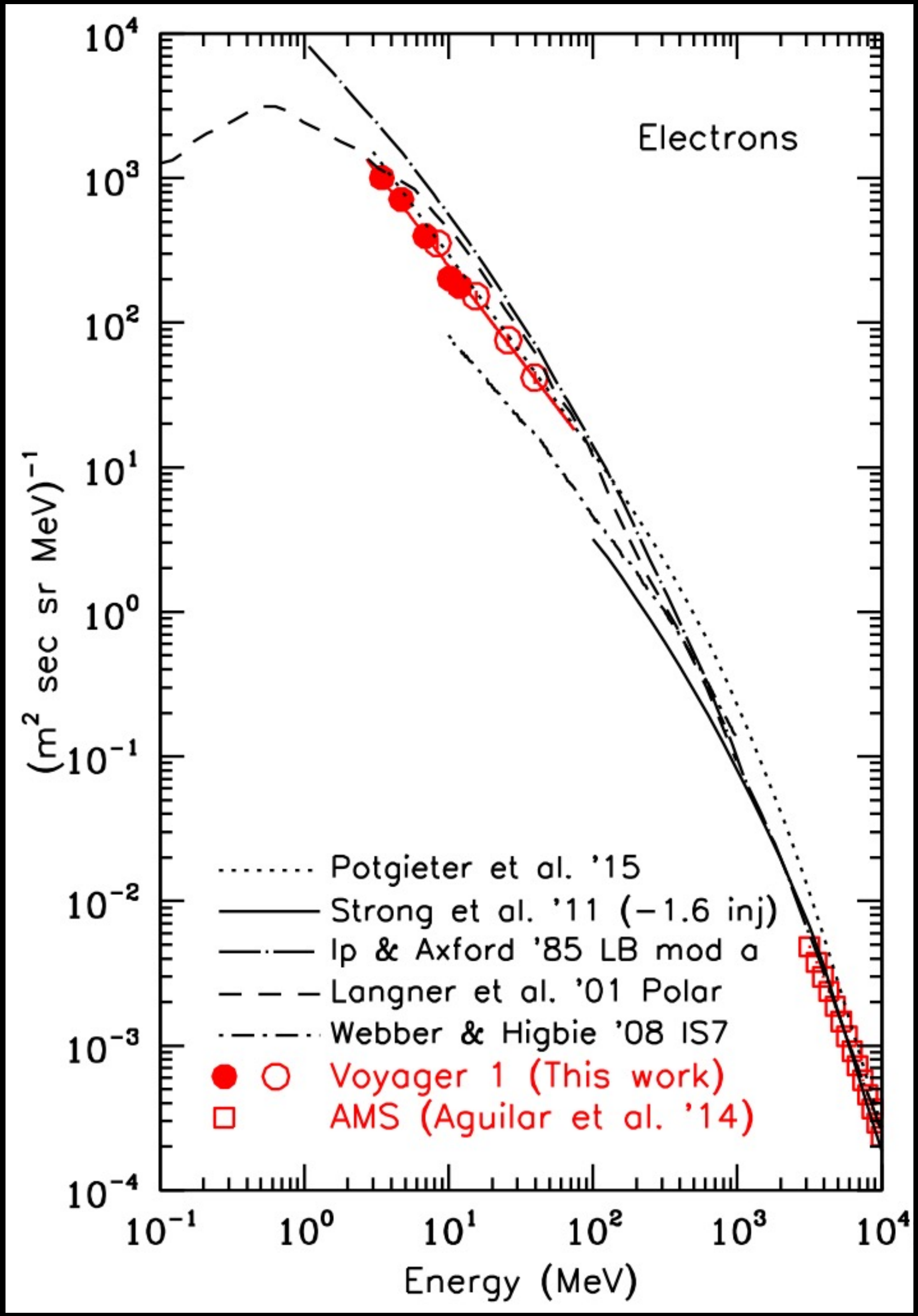

Cummings+ (2016)

Magnetic field:
- in the ISM (black lines);
- from the Sun (white lines).

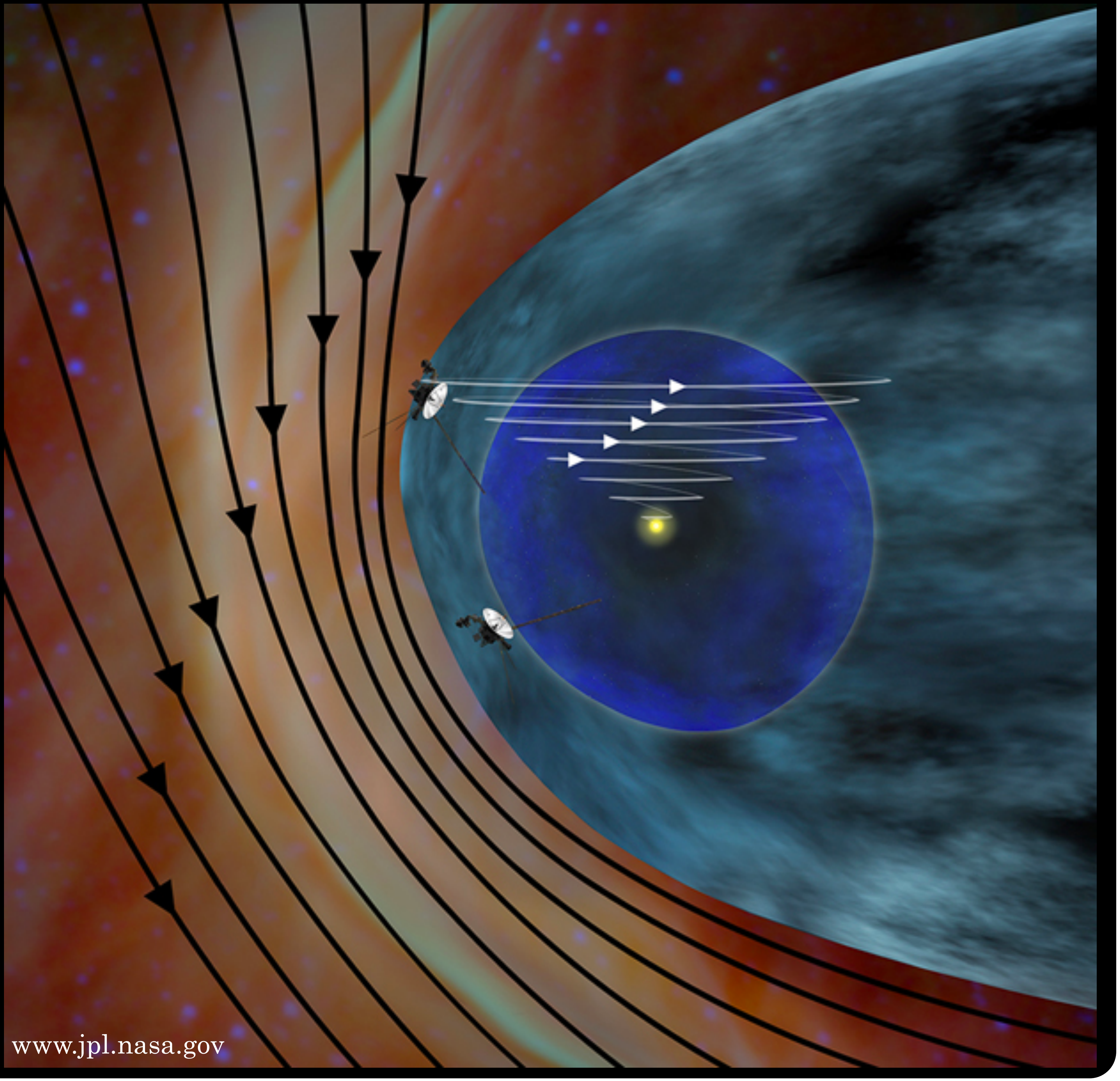
www.jpl.nasa.gov

Next expected signature:
variation in the magnetic field direction

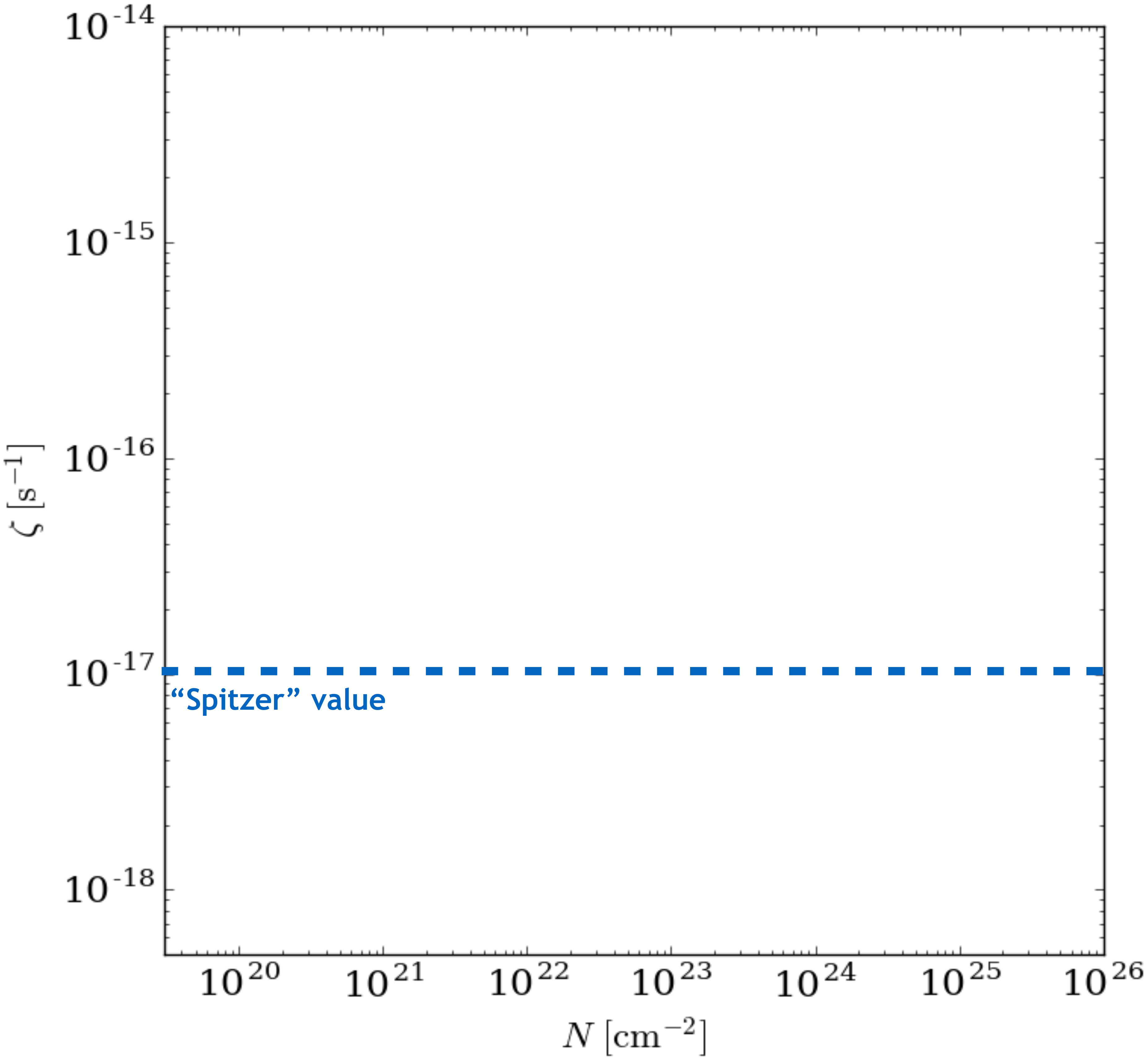
10^{-14}
10^{-15}
10^{-16}
10^{-17}
10^{-18}
ζ [s^{-1}]
10^{20}
10^{21}
10^{22}
10^{23}
10^{24}
10^{25}
10^{26}
N [cm^{-2}]
"Spitzer" value

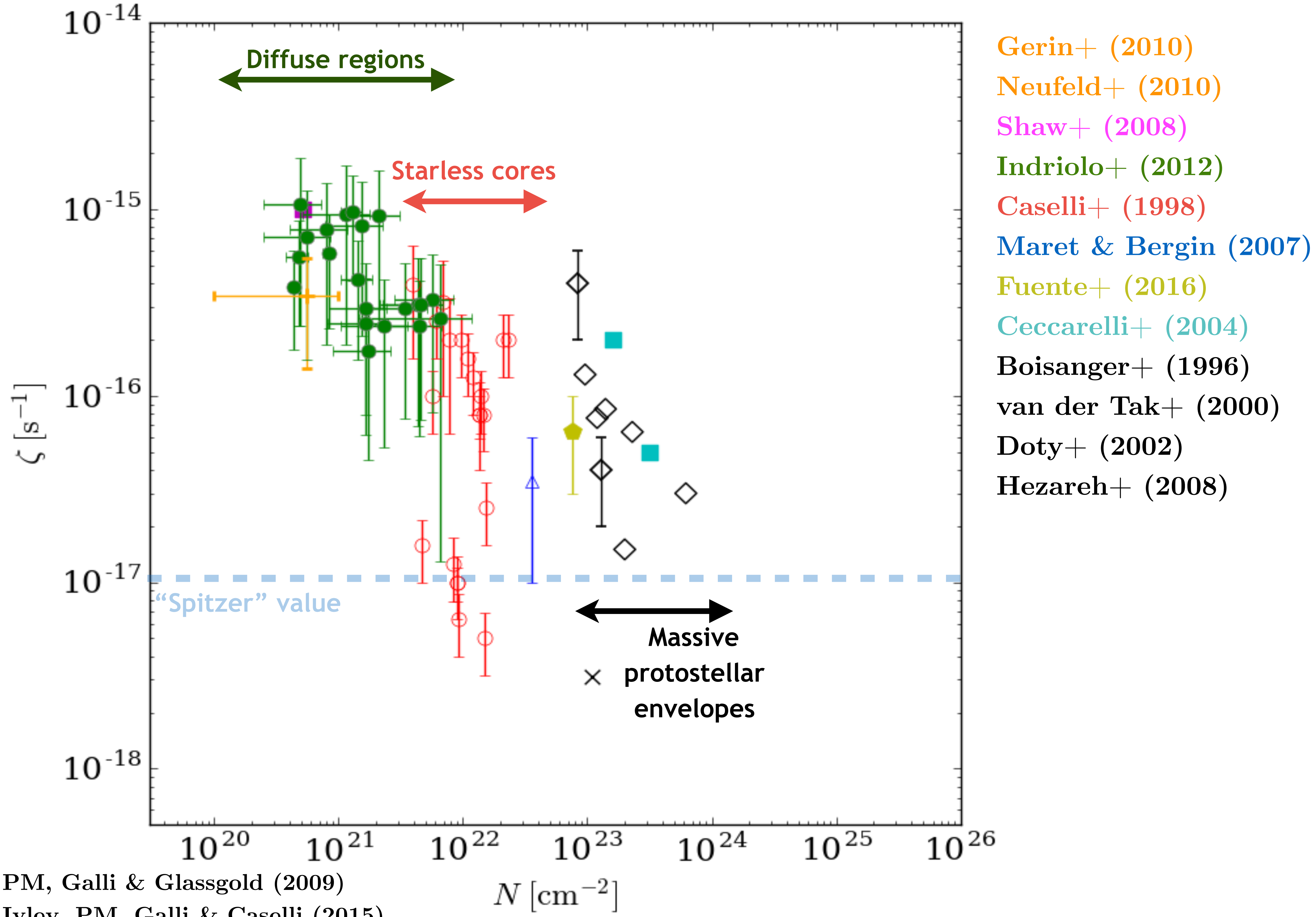

PM, Galli & Glassgold (2009)
Ivlev, PM, Galli & Caselli (2015)

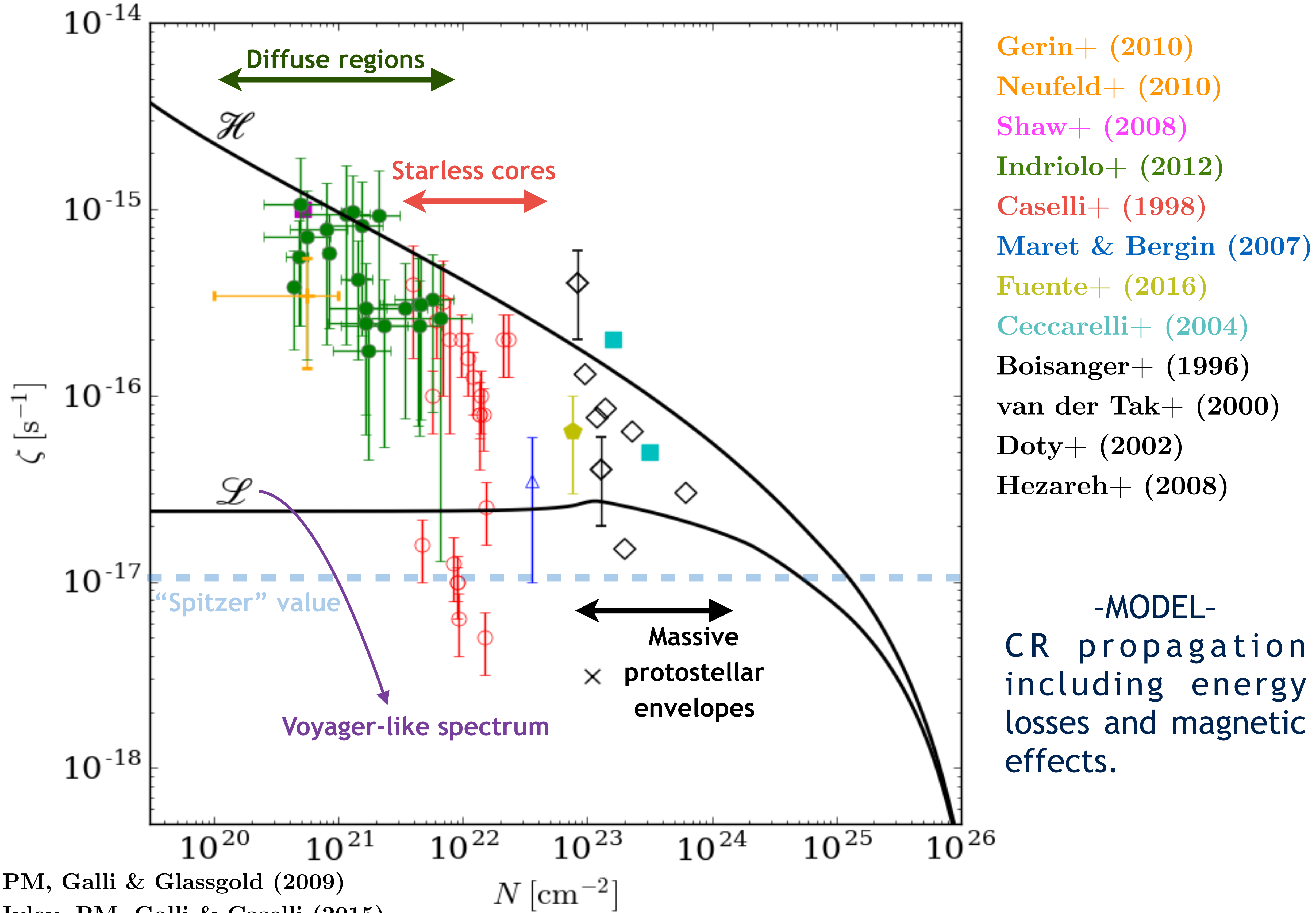

-MODEL-

CR propagation including energy losses and magnetic effects.

PM, Galli & Glassgold (2009)
Ivlev, PM, Galli & Caselli (2015)

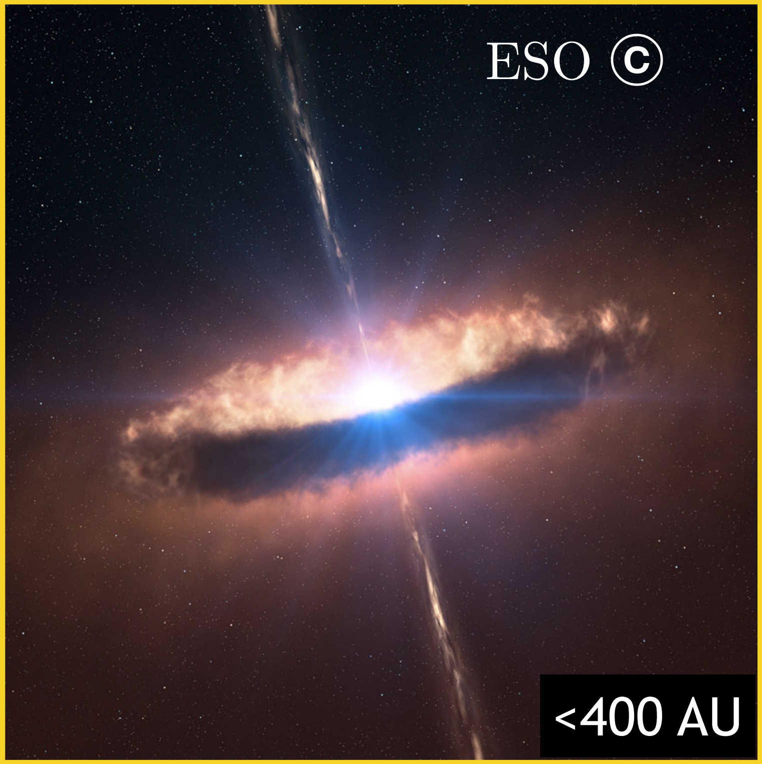

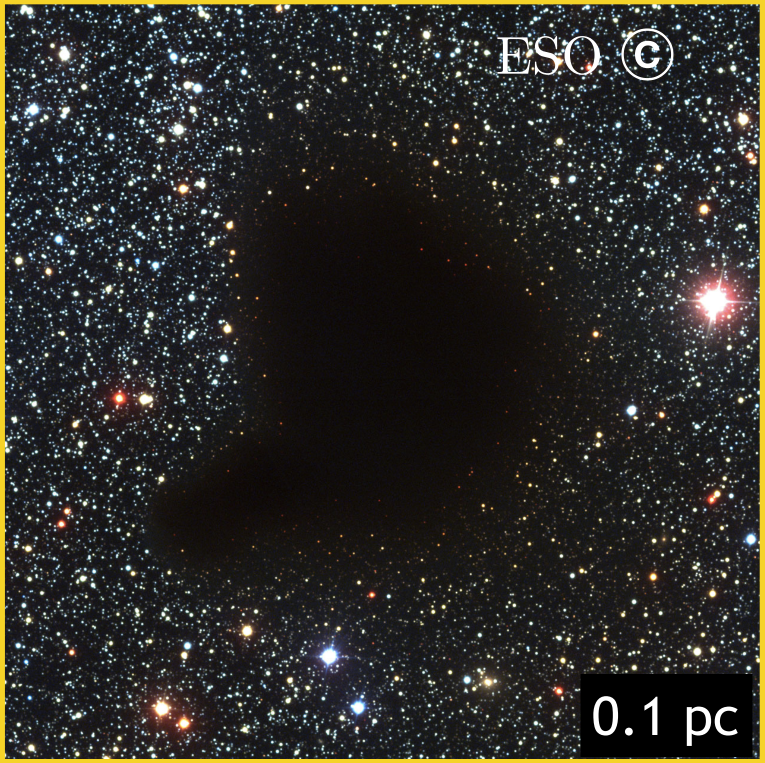

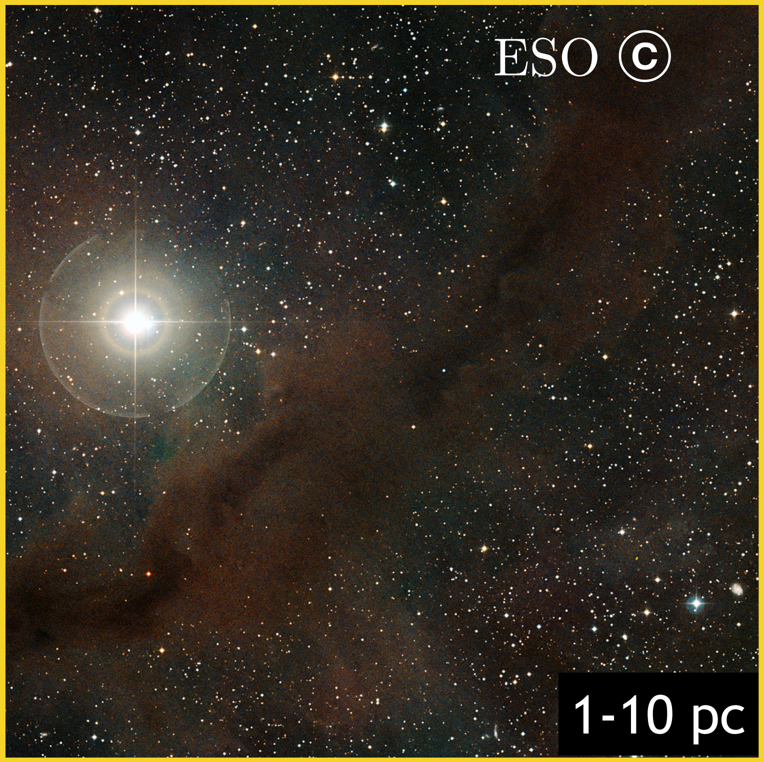

$\approx 10^{-19}$ 10^{-17} 10^{-15}

10^{-22} 10^{-18} 10^{-16}

protostar dense diffuse

$\zeta\ [\mathrm{s}^{-1}]$

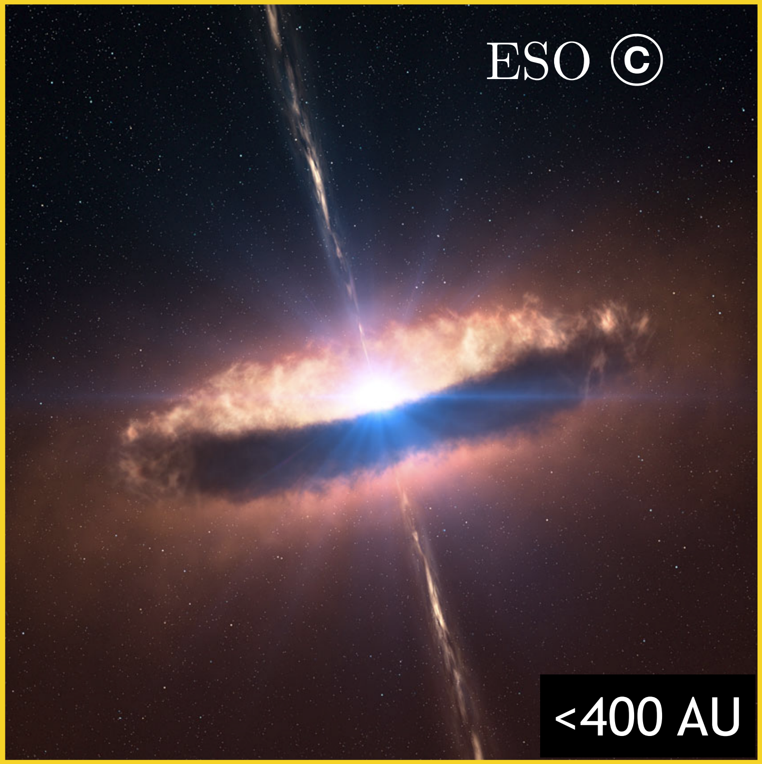

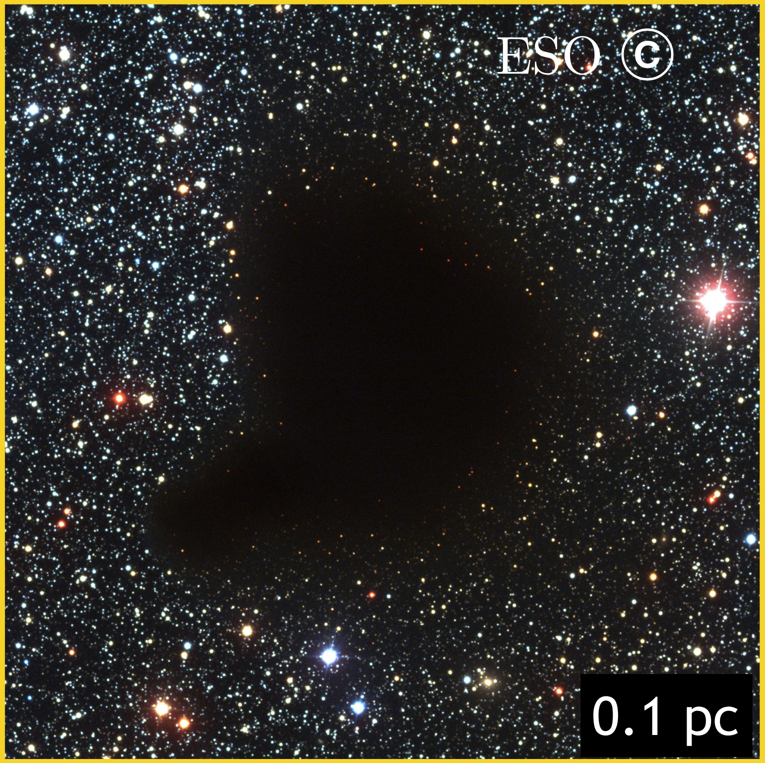

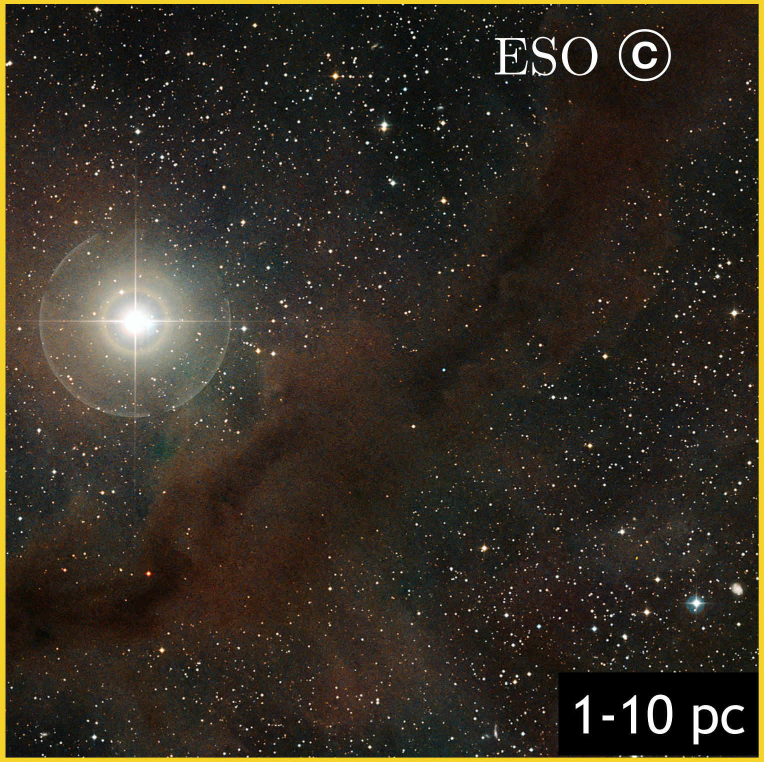

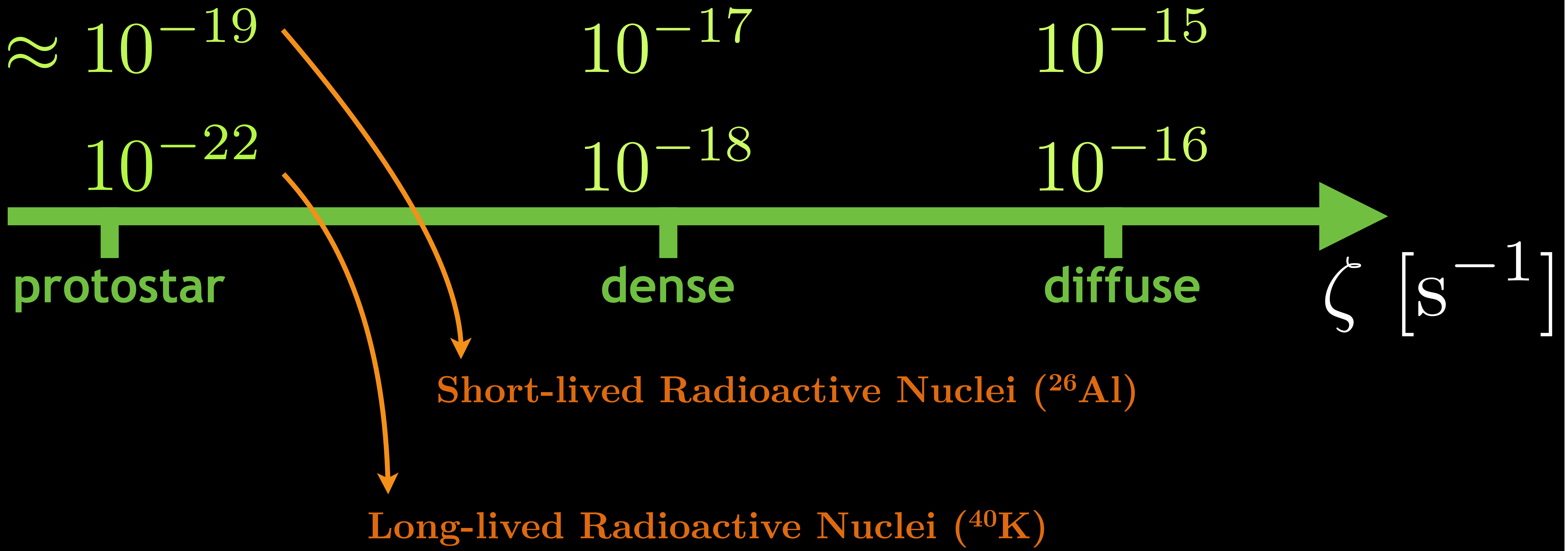

$\approx 10^{-19}$ 10^{-17} 10^{-15}

10^{-22} 10^{-18} 10^{-16}

protostar **dense** **diffuse** $\zeta\ [\mathrm{s}^{-1}]$

Short-lived Radioactive Nuclei (^{26}Al)

Long-lived Radioactive Nuclei (^{40}K)

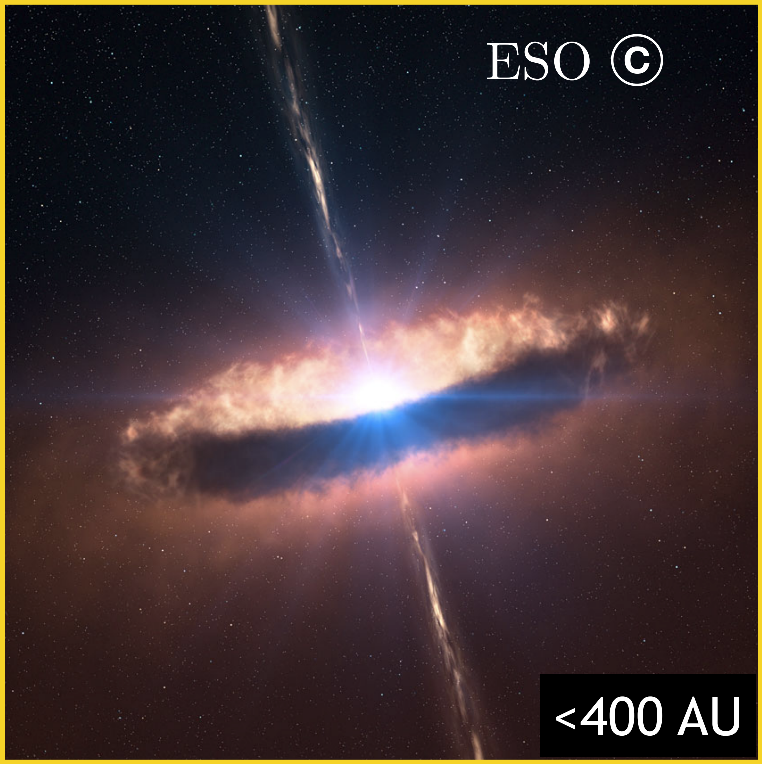

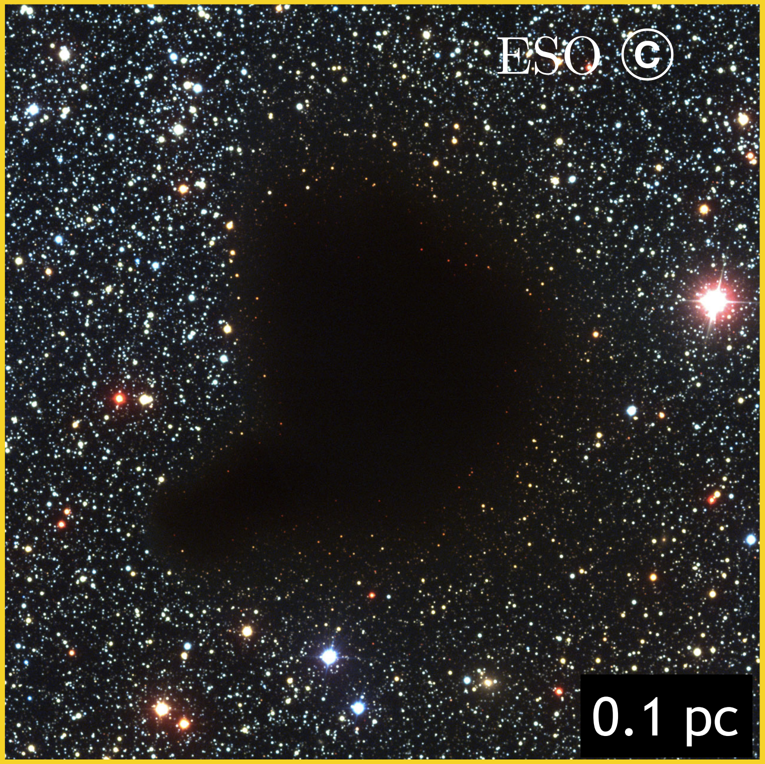

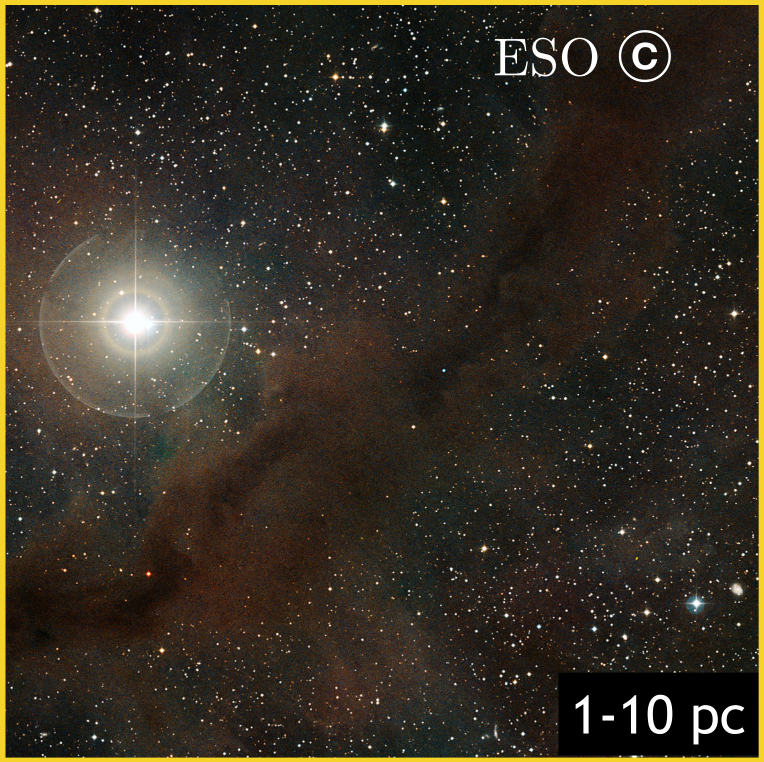

ζ~3×10^{-16} s^{-1} in L1157-B1 (Podio+ 2014)

ζ~4×10^{-14} s^{-1} and 8×10^{-12} s^{-1} in OMC-2 FIR 4 (Ceccarelli+ 2014)

$S_\nu \propto \nu^{-0.89\pm0.07}$ in the bow shock of DG Tau (Ainsworth+ 2014)

CR propagation in 3D simulations of collapsing rotating core

Intermediate magnetisation $\lambda=5$

Perpendicular rotator $(\mathbf{J},\mathbf{B})=\pi/2$

Field lines in the inner 600 AU

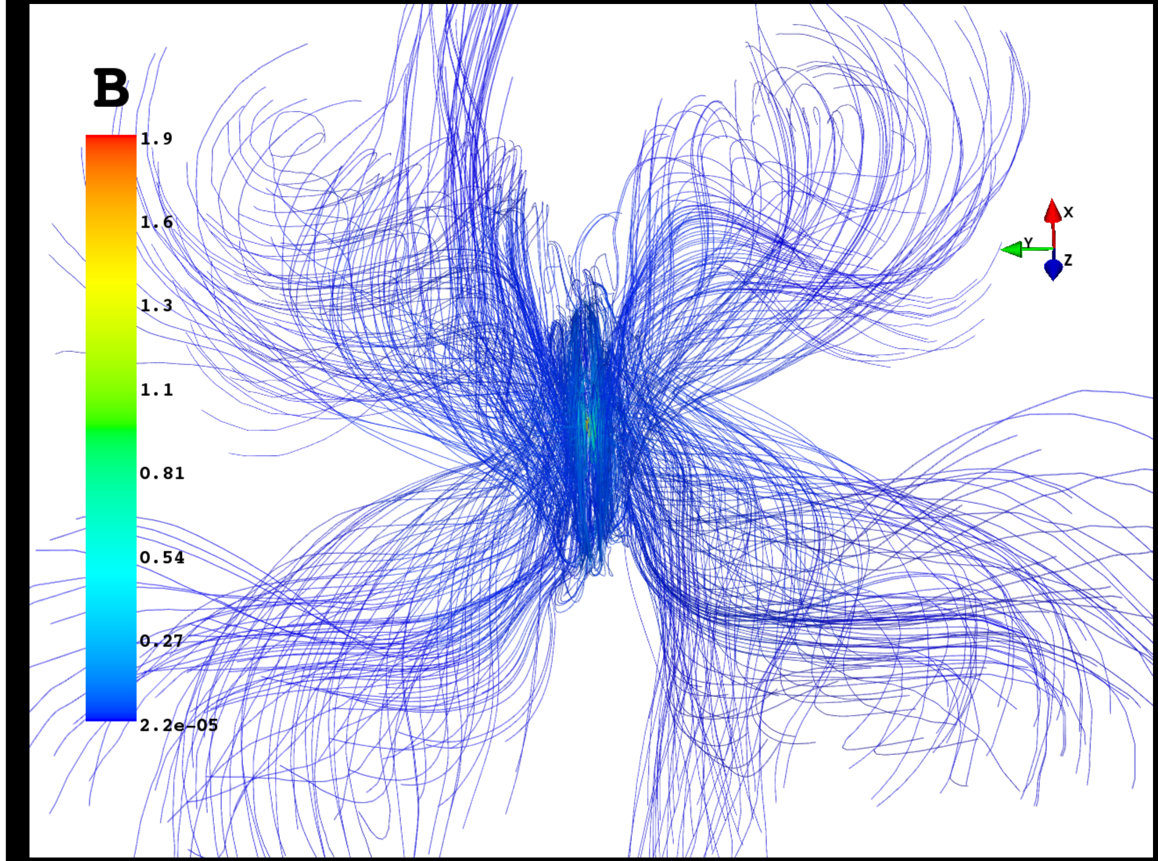

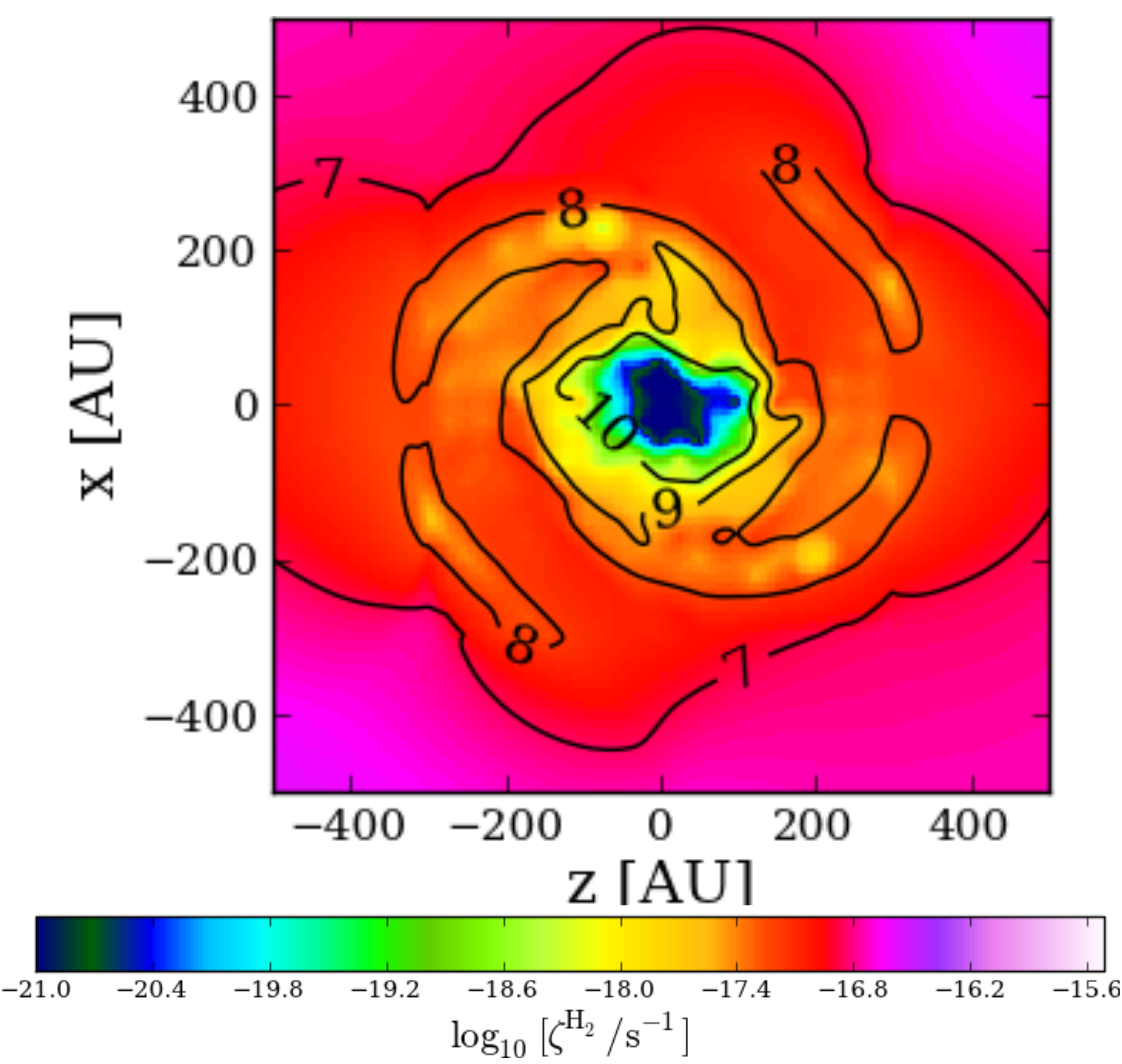

PM, Hennebelle & Galli (2013)

$\approx 10^{-19}$

10^{-22}

protostar

ζ~3×10^{-16} s^{-1} in L1157-B1 (Podio+ 2014)

ζ~4×10^{-14} s^{-1} and 8×10^{-12} s^{-1} in OMC-2 FIR 4 (Ceccarelli+ 2014)

$S_\nu \propto \nu^{-0.89\pm0.07}$ in the bow shock of DG Tau (Ainsworth+ 2014)

What are the possible sources of energetic particles?

Padovani+ (2016)

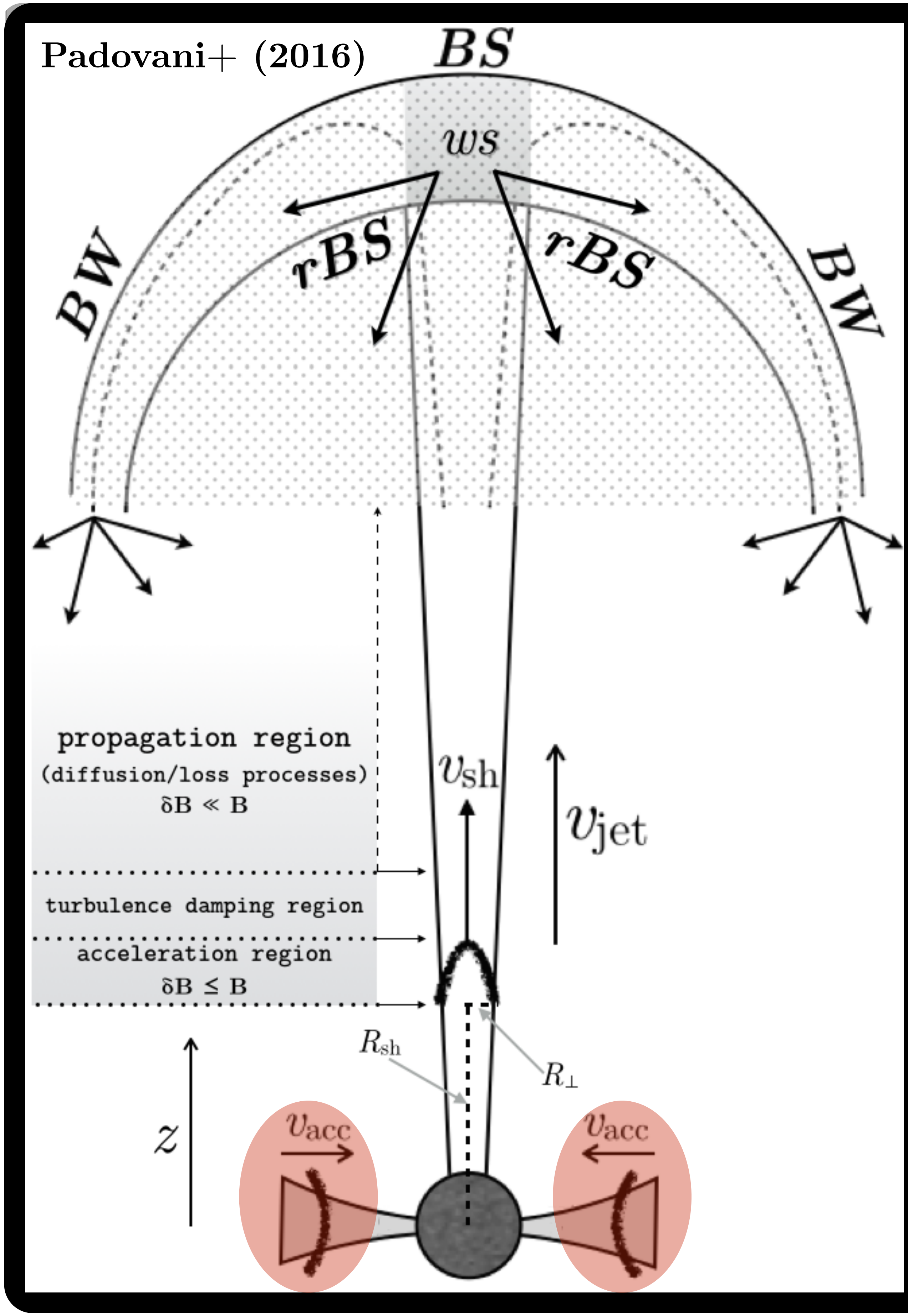

Acceleration sites

(1) accretion flows;

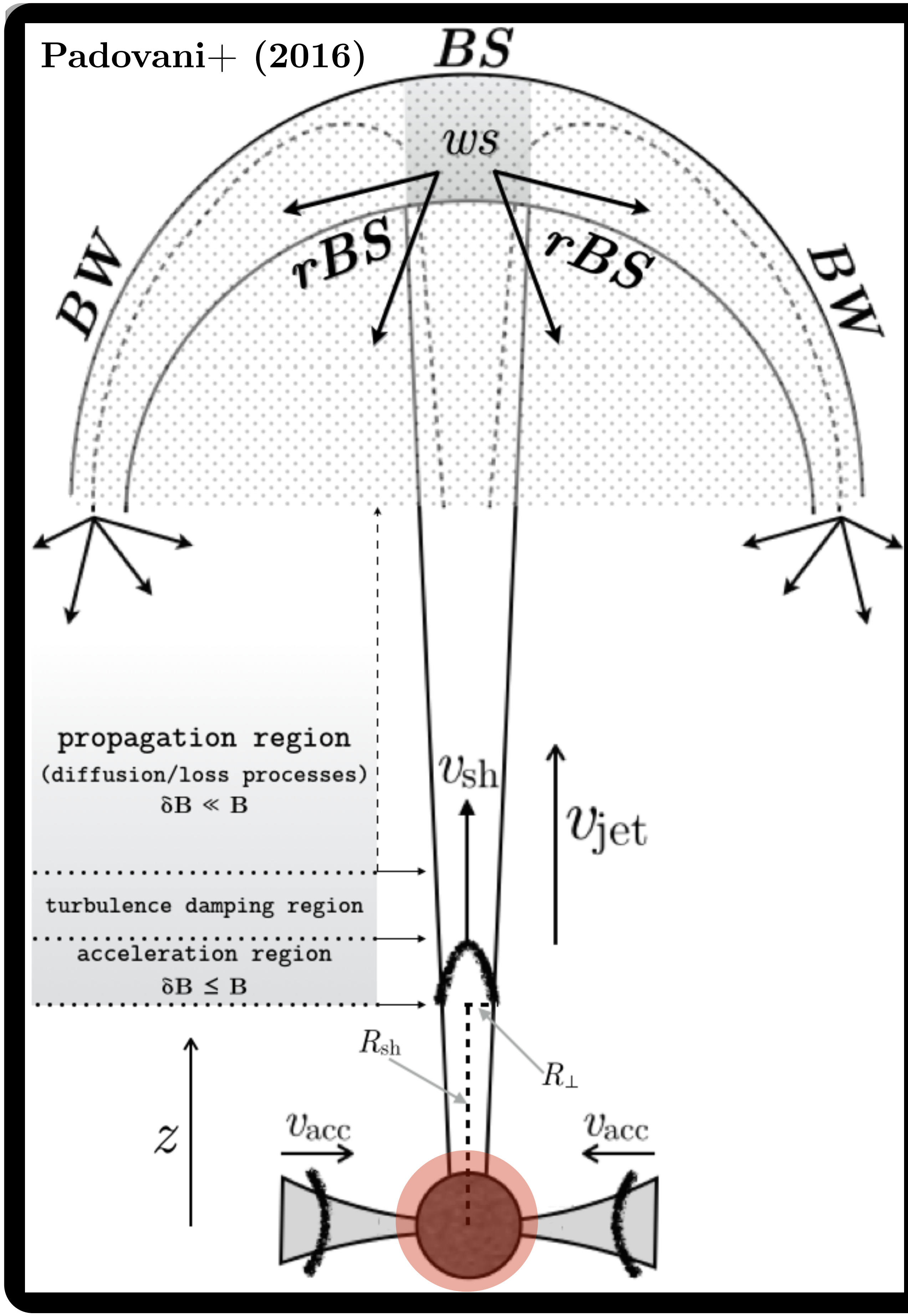
Padovani+ (2016)

Acceleration sites

(1) accretion flows;

(2) protostellar surface;

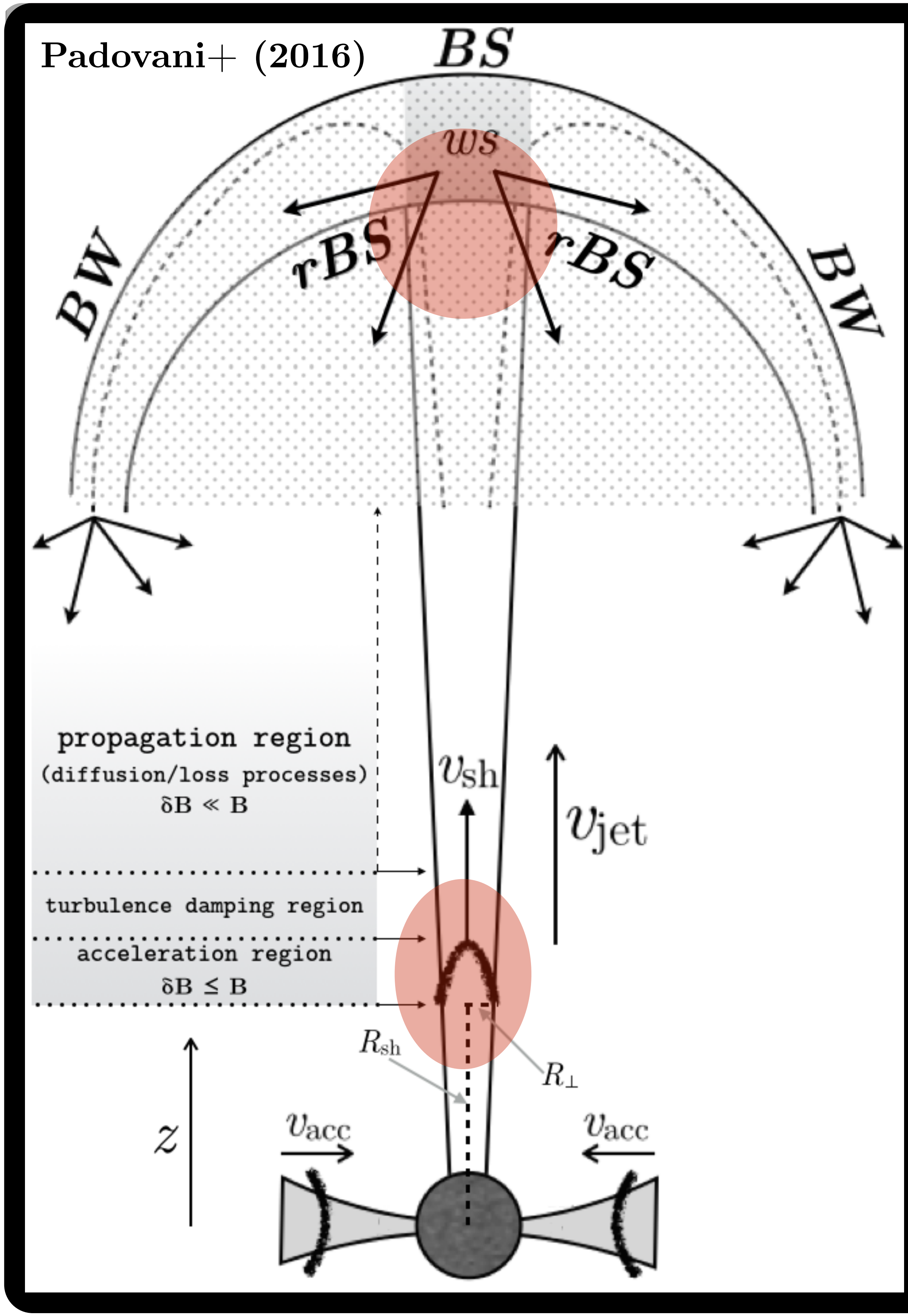

Acceleration sites

(1) accretion flows;

(2) protostellar surface;

(3) jet shock;

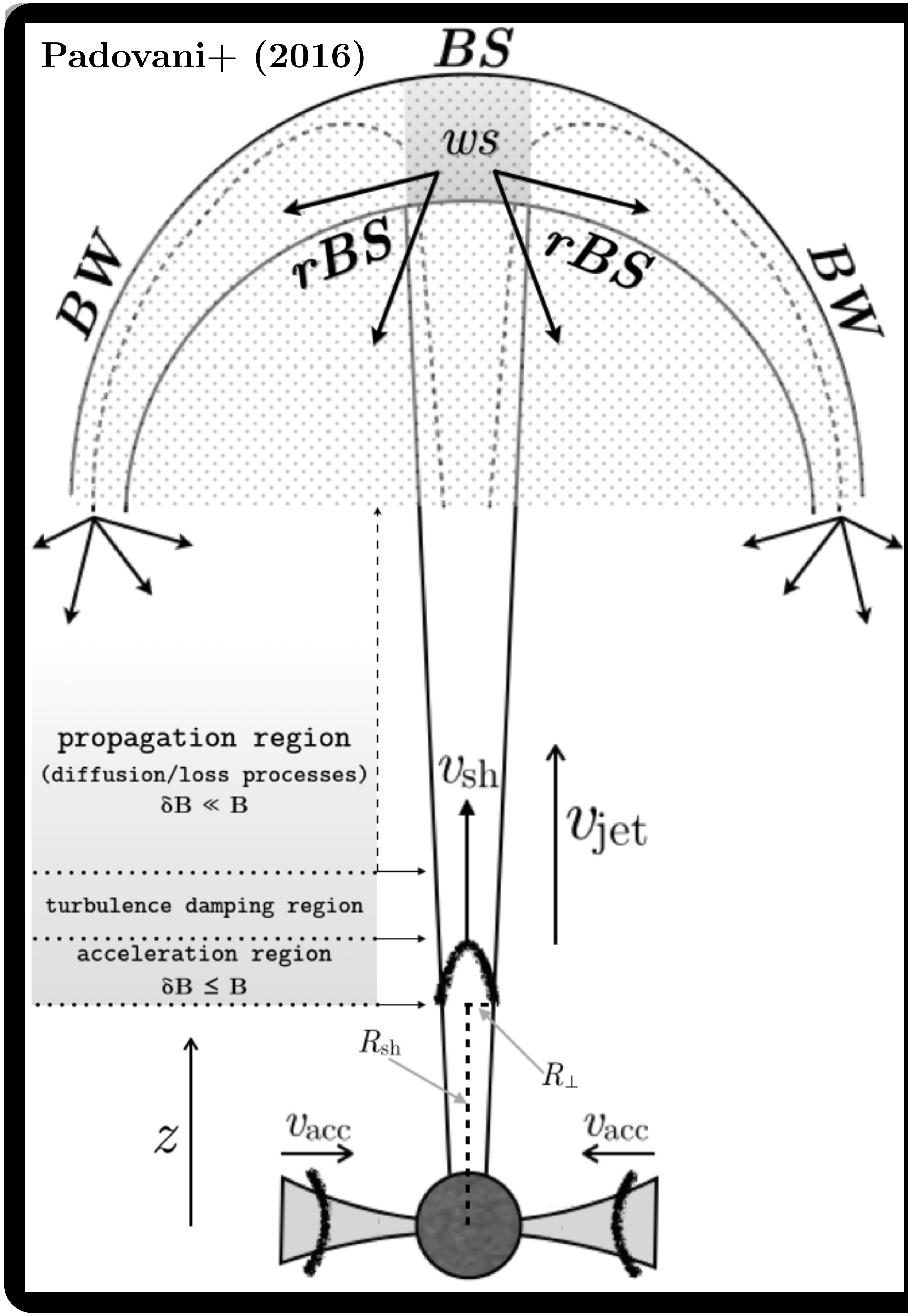
Padovani+ (2016)

Acceleration sites

(1) accretion flows;
(2) protostellar surface;
(3) jet shock;

Diffusive Shock Acceleration (DSA) or
First-order Fermi acceleration

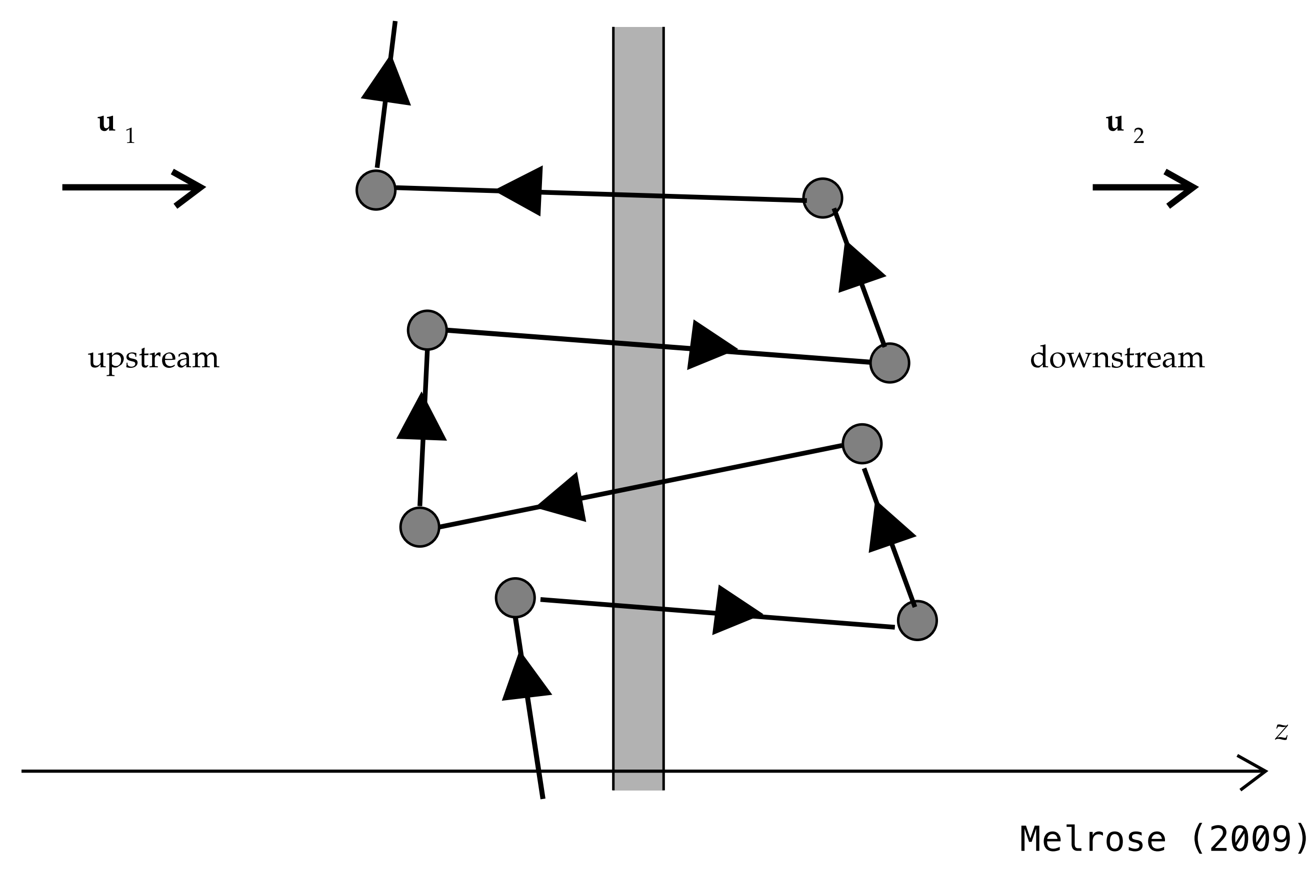
Melrose (2009)

Conditions to be fulfilled

Condition on flow velocity: **supersonic** and **super-Alfvénic**.

(1) **acceleration time shorter** than **collisional loss time**;

(2) **acceleration time shorter** than **dynamical time**;

(3) **shock geometry**: particles have to be accelerated before they start to escape by diffusion processes.

Presence of an ***incomplete ionised medium***: neutrals can decrease the effectiveness of the DSA mechanism damping the particle's self-generated Alfvén waves that are responsible of the particle scattering back and forth the shock (Drury+ 1996).

$$t_{\rm acc} = \min(t_{\rm loss}, t_{\rm esc,u}, t_{\rm esc,d}, t_{\rm dyn}) \to E_{\rm max}$$

Parameters needed for the model

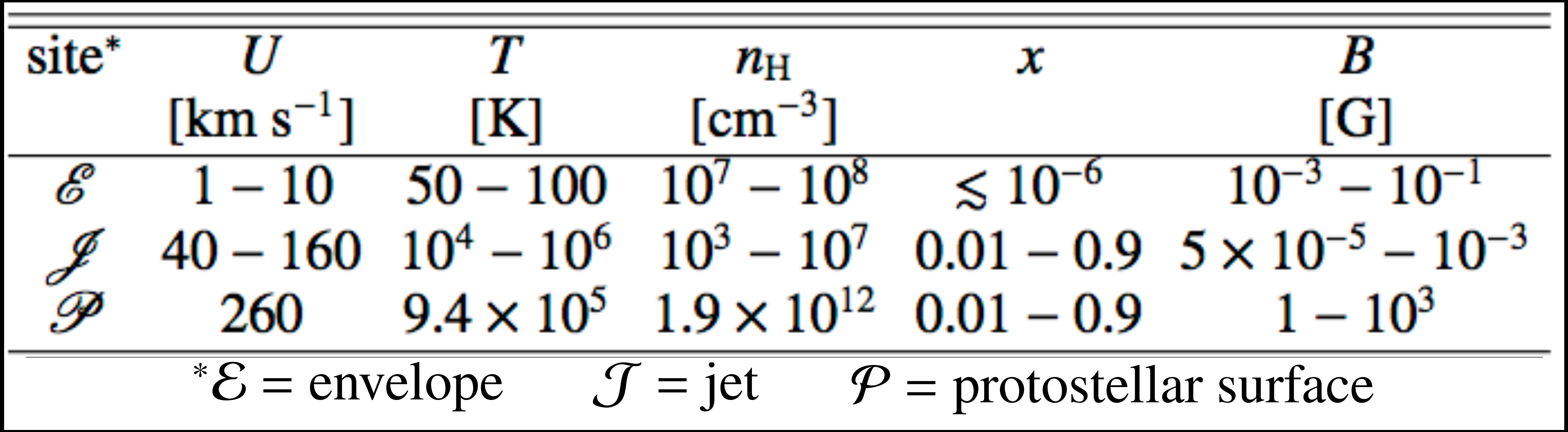

site*	U [km s^{-1}]	T [K]	$n_{\rm H}$ [cm^{-3}]	x	B [G]
$\mathscr{E}$	$1-10$	$50-100$	10^7-10^8	$\lesssim 10^{-6}$	$10^{-3}-10^{-1}$
$\mathscr{J}$	$40-160$	10^4-10^6	10^3-10^7	$0.01-0.9$	$5\times10^{-5}-10^{-3}$
$\mathscr{P}$	260	9.4×10^5	1.9×10^{12}	$0.01-0.9$	$1-10^3$

*$\mathcal{E}$ = envelope $\mathcal{J}$ = jet $\mathcal{P}$ = protostellar surface

Refs: $U_{\rm sh}$ (Raga+ 2002,2011; Hartigan & Morse 2007; Agra-Amboage+ 2011);
T (Frank+ 2014);
$n_{\rm H}$ (Lefloch+ 2012; Gómez-Ruiz+ 2012);
x (Nisini+ 2005; Podio+ 2006; Antoniucci+ 2008; Garcia López+ 2008; Dionatos+ 2010; Frank+ 2014; Maurri+ 2014);
B (Tesileanu+ 2009, 2012)
For protostellar surface shock, parameters from Masunaga & Inutsuka (2000)

- DSA works *only* for protons (electrons lose energy too fast, $E^{\rm max}(e)$<300 MeV);
- DSA is effective *only* in jet and protostellar surface shocks (in accretion flows, x and U_{sh} are too small, quenching the particle acceleration; B is as large as to produce a sub-Alfvénic shock).

Maximum Energy

$$t_{\rm acc} = \min(t_{\rm loss}, t_{\rm esc,u}, t_{\rm esc,d}, t_{\rm dyn}) \rightarrow E_{\rm max}$$

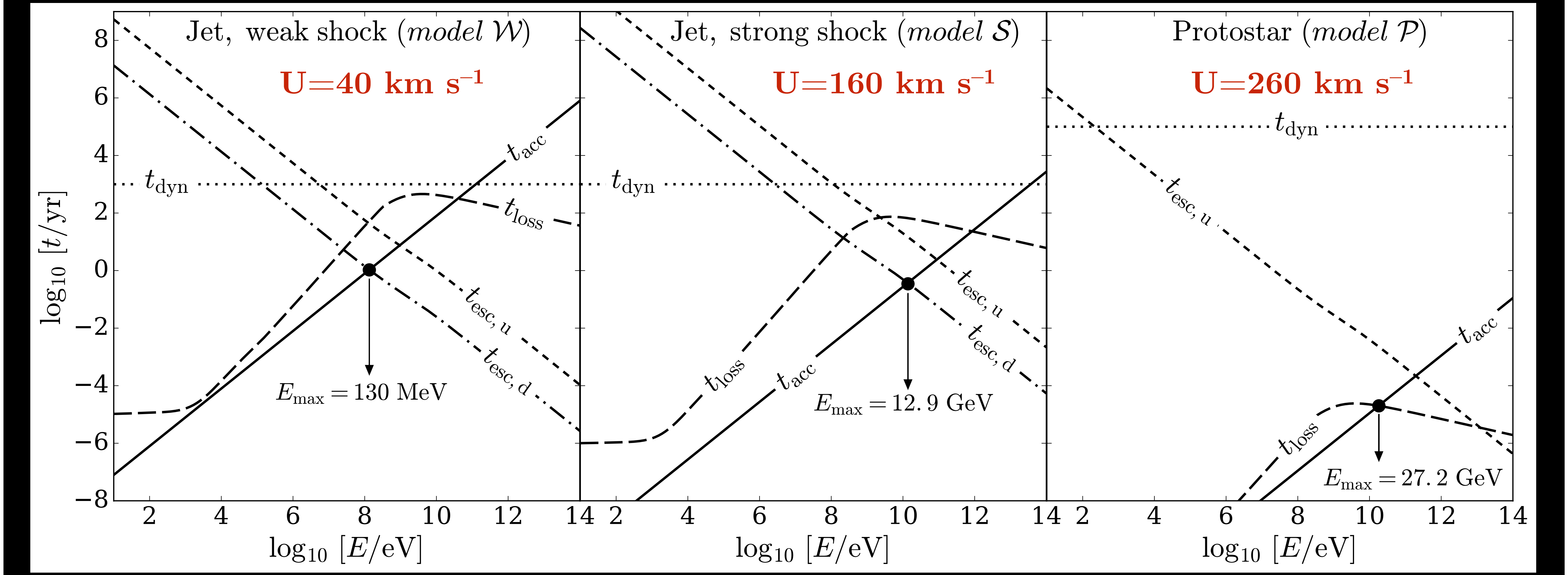

PM, Marcowith, Hennebelle & Ferrière (2017)

Application of the modelling: comparison with available observations

Ainsworth+ (2014) detected synchrotron emission (GMRT) towards the bow shock (knot C) of DG Tau, speculating that this could be due to relativistic electrons accelerated in the interaction between the jet and the ambient medium.

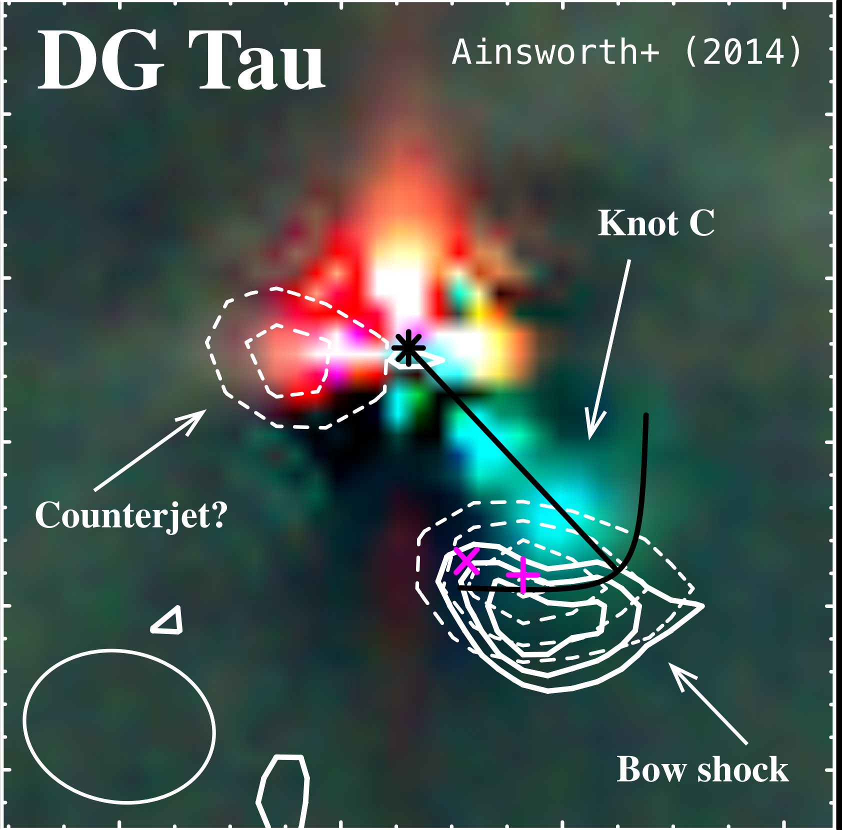

325 MHz (solid contours);
610 MHz (dashed contours).

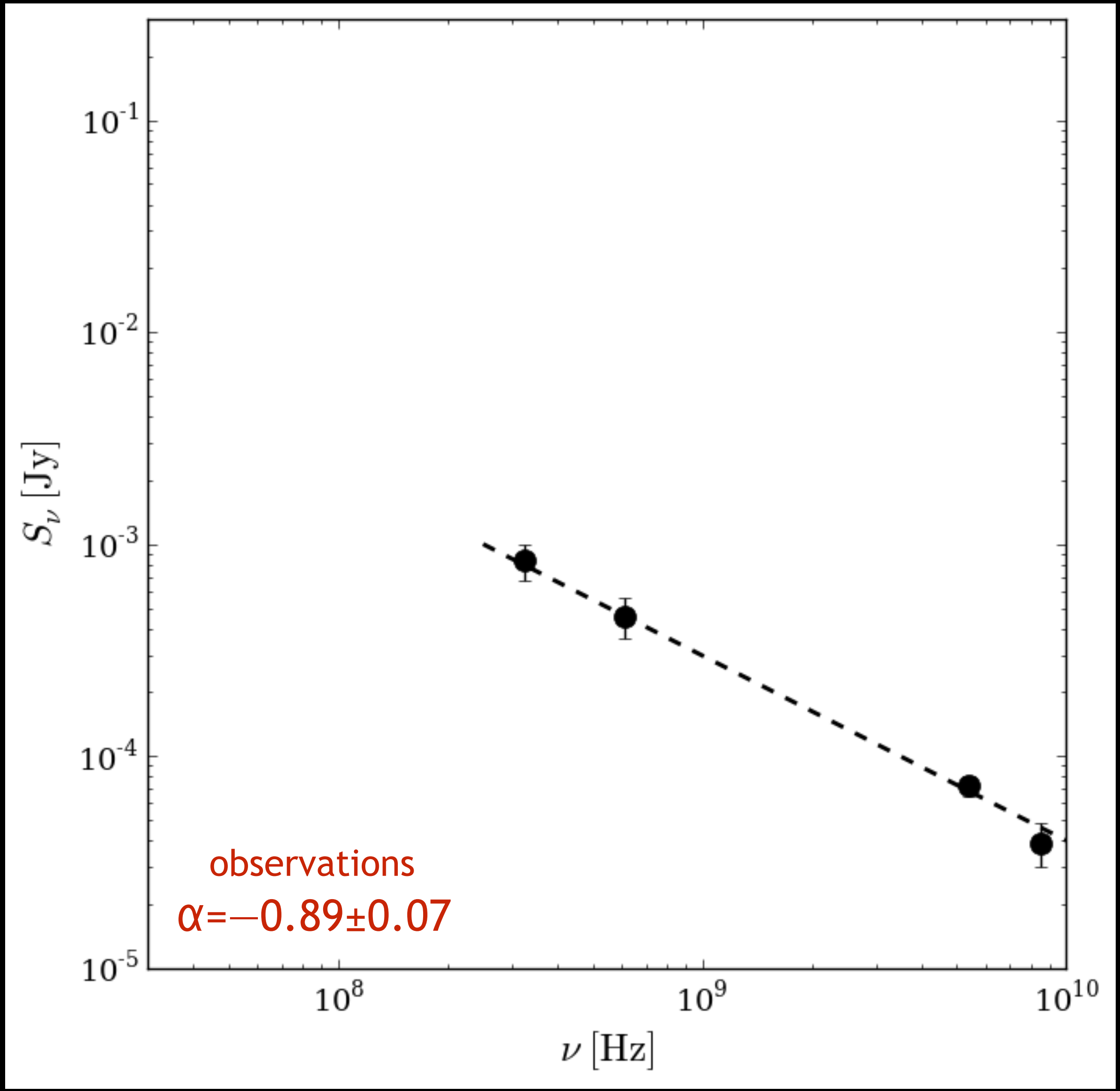

Using results by Lynch+ (2013), EVLA obs.

Application of the modelling: comparison with available observations

Ainsworth+ (2014) detected synchrotron emission (GMRT) towards the bow shock (knot C) of DG Tau, speculating that this could be due to relativistic electrons accelerated in the interaction between the jet and the ambient medium.

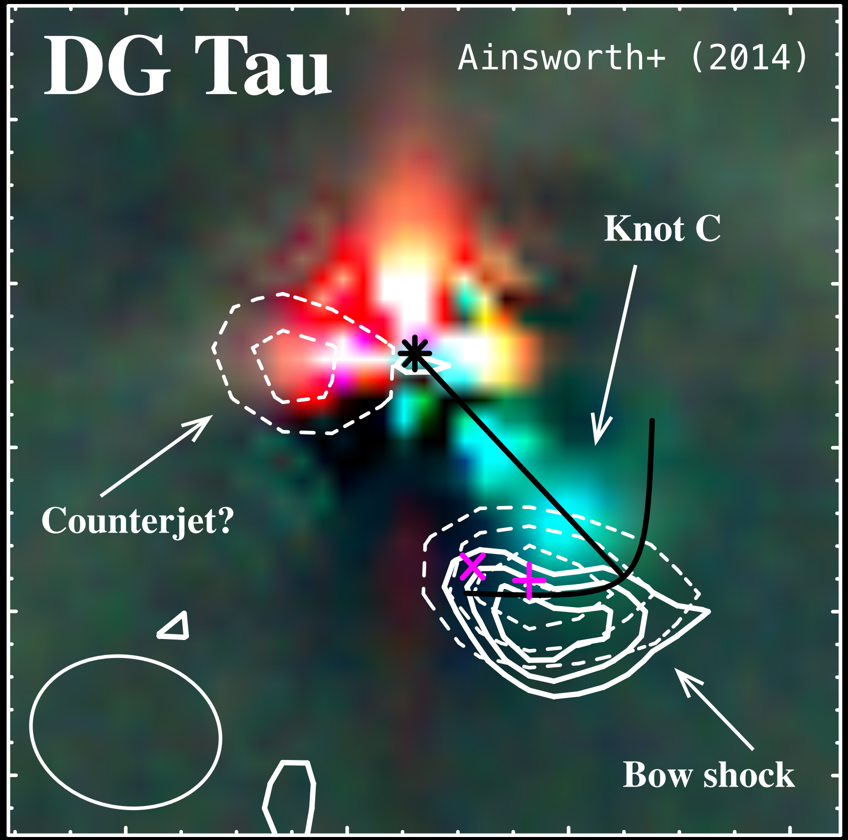

325 MHz (solid contours);
610 MHz (dashed contours).

Using results by Lynch+ (2013), EVLA obs.

- kinematic and physical properties along the jet (McGroarty+ 2009; Oh+ 2015);
- Hypothesis: first acceleration at knot B (Eislöffel & Mundt 1998) plus a re-acceleration at knot C.

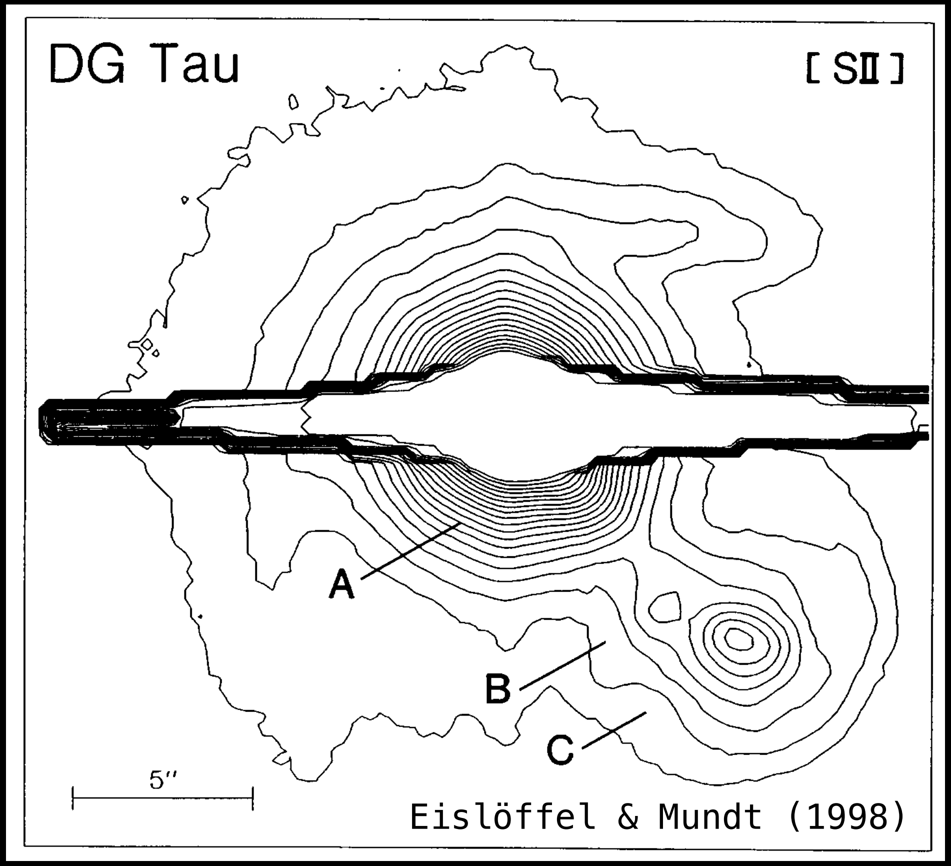

Application of the modelling: comparison with available observations

Ainsworth+ (2014) detected synchrotron emission (GMRT) towards the bow shock (knot C) of DG Tau, speculating that this could be due to relativistic electrons accelerated in the interaction between the jet and the ambient medium.

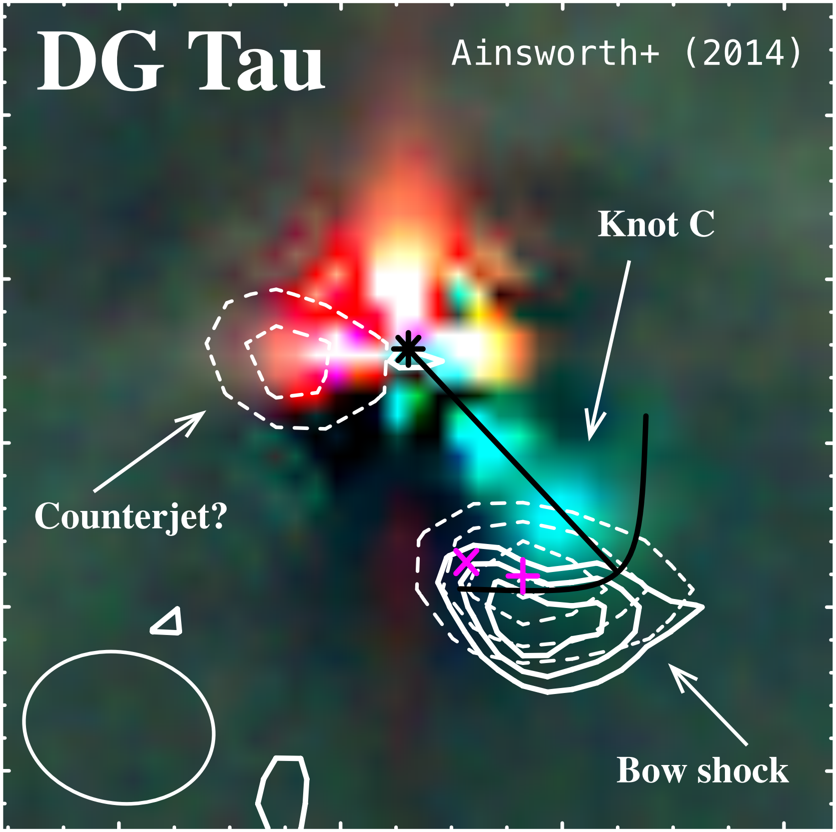

325 MHz (solid contours);
610 MHz (dashed contours).

Using results by Lynch+ (2013), EVLA obs.

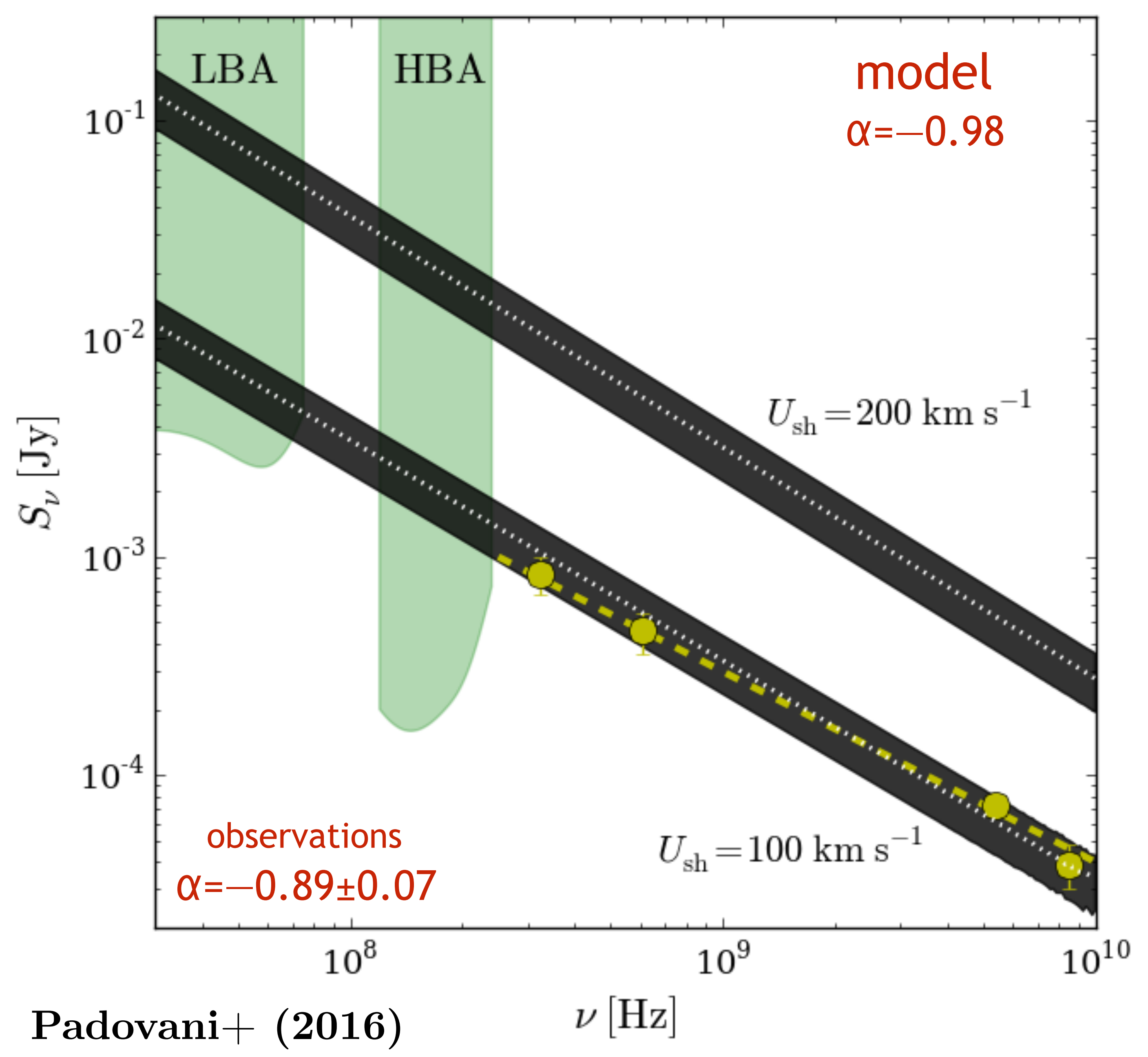

Padovani+ (2016)

Application of the modelling: comparison with available observations

Ainsworth+ (2014) detected synchrotron emission (GMRT) towards the bow shock (knot C) of DG Tau, speculating that this could be due to relativistic electrons accelerated in the interaction between the jet and the ambient medium.

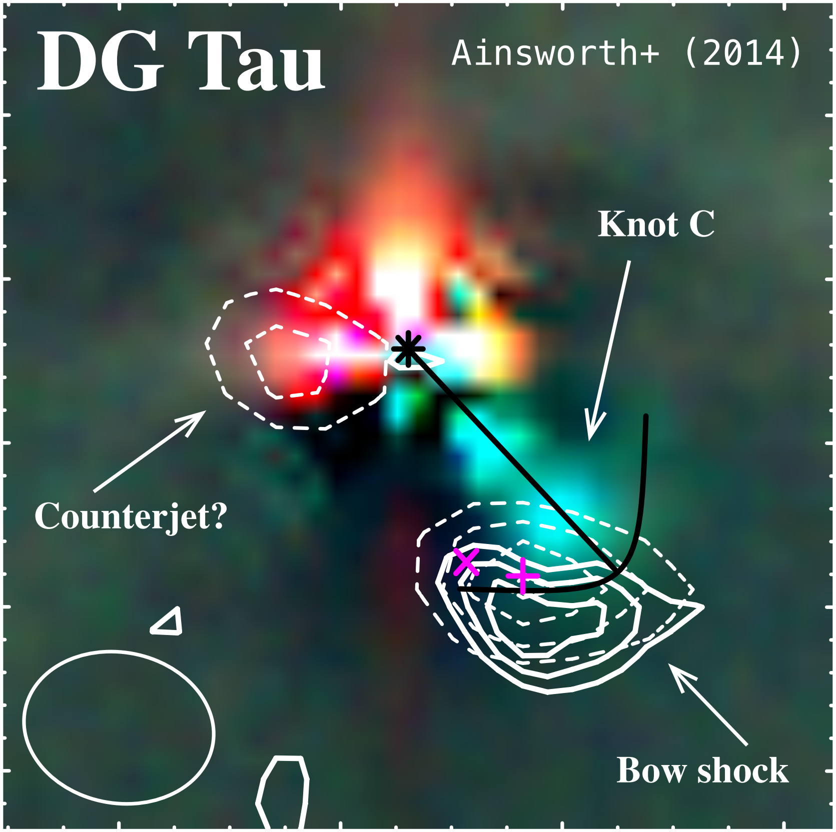

325 MHz (solid contours);
610 MHz (dashed contours).

Using results by Lynch+ (2013), EVLA obs.

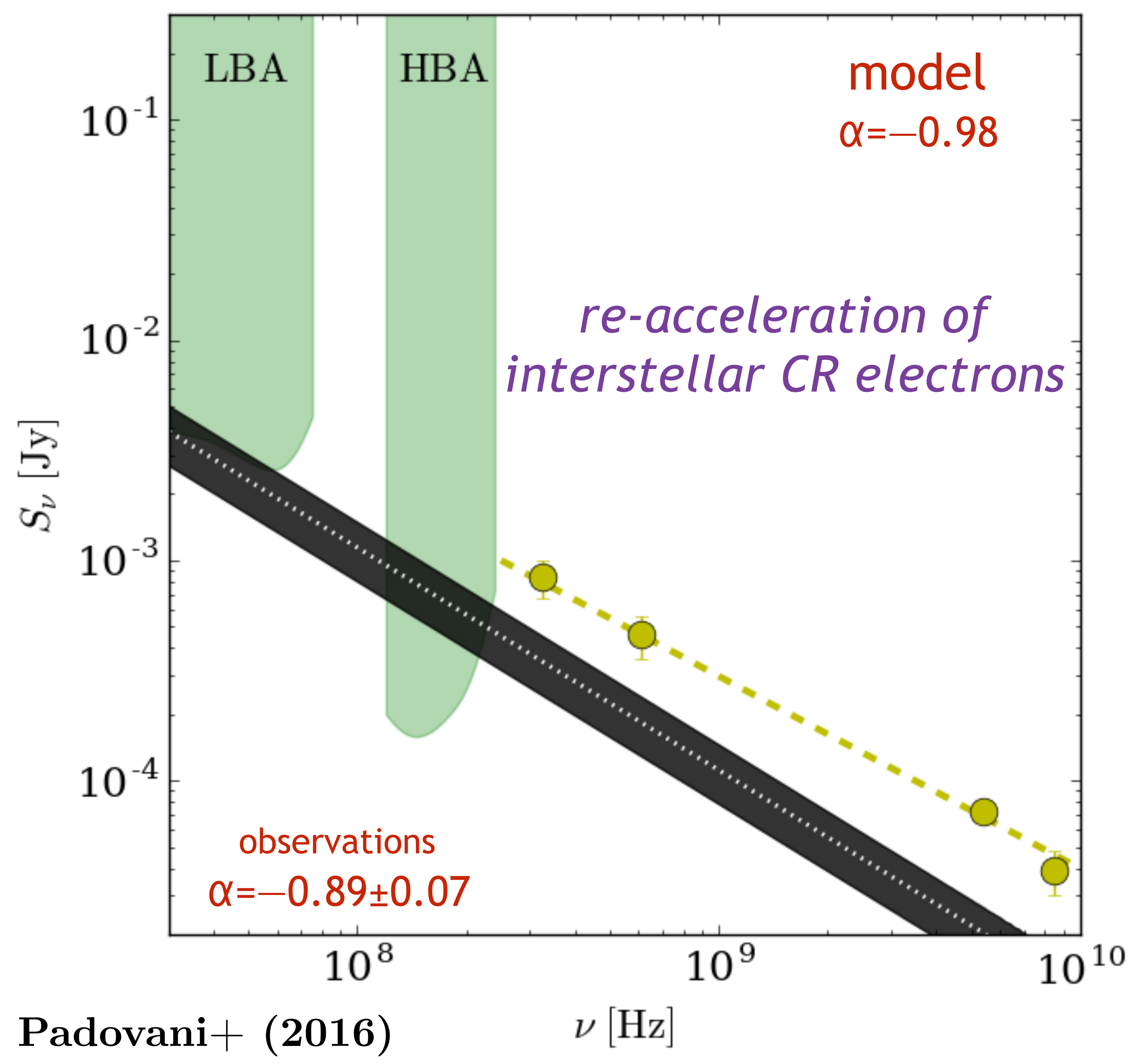

Padovani+ (2016)

Application of the modelling: comparison with available observations

Podio+ (2014): $\zeta=3\times10^{-16}$ s^{-1} in the bow shock B1 in L1157 (HCO^+, N_2H^+).

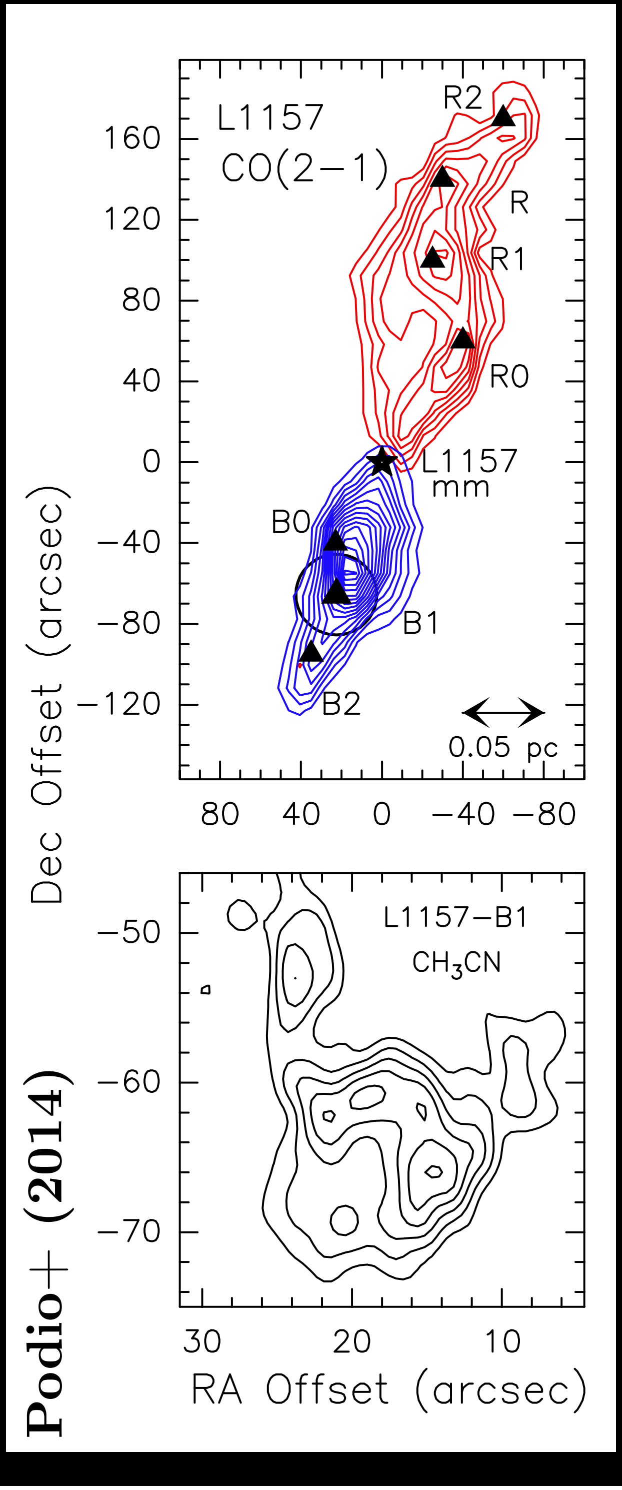

Podio+ (2014)

- Youngest knot B0 at 1.2×10^3 AU; B1 at 1.7×10^4 AU with an hot-spot cavity radius of 1.2×10^3 AU (Lefloch+ 2012);
- source distance: 250 pc (Looney+ 2007);
- $v_{flow}\approx100$ km s^{-1}, v_{jet}=20-40 km s^{-1} (Bachiller+ 2001; Tafalla+ 2015);
- $n_H=10^5$-10^6 cm^{-3} (Gómez-Ruiz+ 2015);
- embedded source, T=60-200 K (Podio+ 2014), but hints of T=10^3 K (Busquet+ 2014) to explain water lines.

Our modelling: $\zeta=6.1\times10^{-16}$ s^{-1}

The values of *all parameters* can vary along the shock surfaces B0 and B1, this is why our result has to be interpreted as a proof of concept.

Need of polarimetric observations (ALMA) to constrain B configuration

Application of the modelling: comparison with available observations

Podio+ (2014): $\zeta=3\times10^{-16}\ \mathrm{s}^{-1}$ in the bow shock B1 in L1157 (HCO^+, N_2H^+).

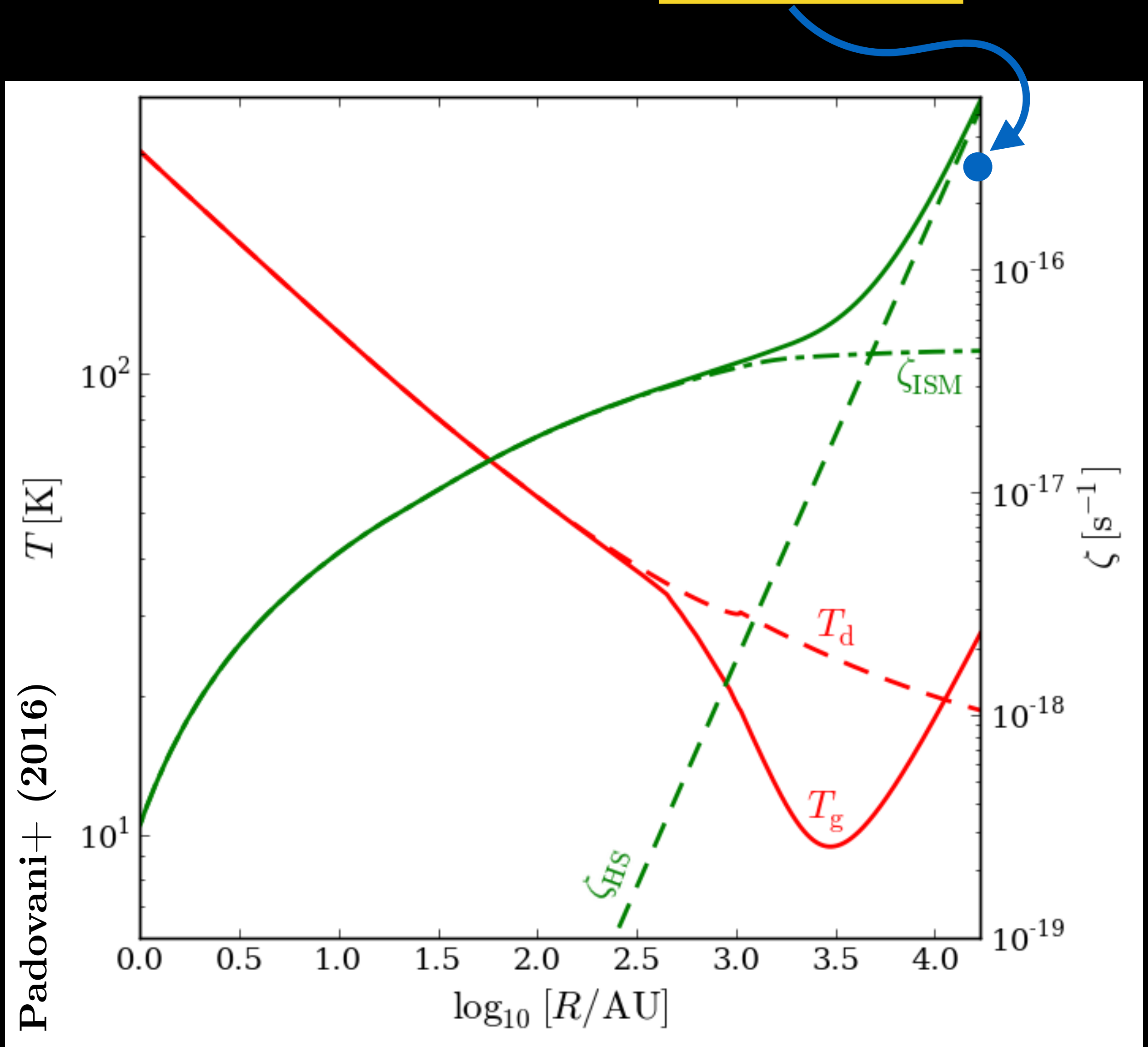

Padovani+ (2016)

- IS CRs, for a Voyager-like spectrum cannot explain the ionisation rate observed;
- the contribution of the hot spot CR flux become negligible at $R<5\times10^3$ AU (geometric dilution factor).

Check on gas temperature, accounting only for the heating due to IS and locally generated CRs (neglecting UV from ISRF).

$$\frac{T_d(R)}{\mathrm{K}} = 300\left(\frac{R}{\mathrm{AU}}\right)^{-0.41}$$

(Chiang+10,12)

- R<300 AU: gas-dust coupling;
- 300 AU<R<3000 AU: T_g ↓ (IS CR heating weak);
- R>3000 AU: T_g ↑ (hot spot CR heating).

Application of the modelling: comparison with available observations

Ceccarelli+ (2014): $\left\{\begin{array}{l}\zeta=1.5\times10^{-12}\ \mathrm{s}^{-1}\ \text{at 1600 AU}\\ \zeta=4\times10^{-14}\ \mathrm{s}^{-1}\ \text{at 3700 AU}\end{array}\right\}$ in OMC-2 FIR 4 (HCO^+, N_2H^+).

Protostellar surface acceleration model (parameters from Masunaga & Inutsuka 2000).

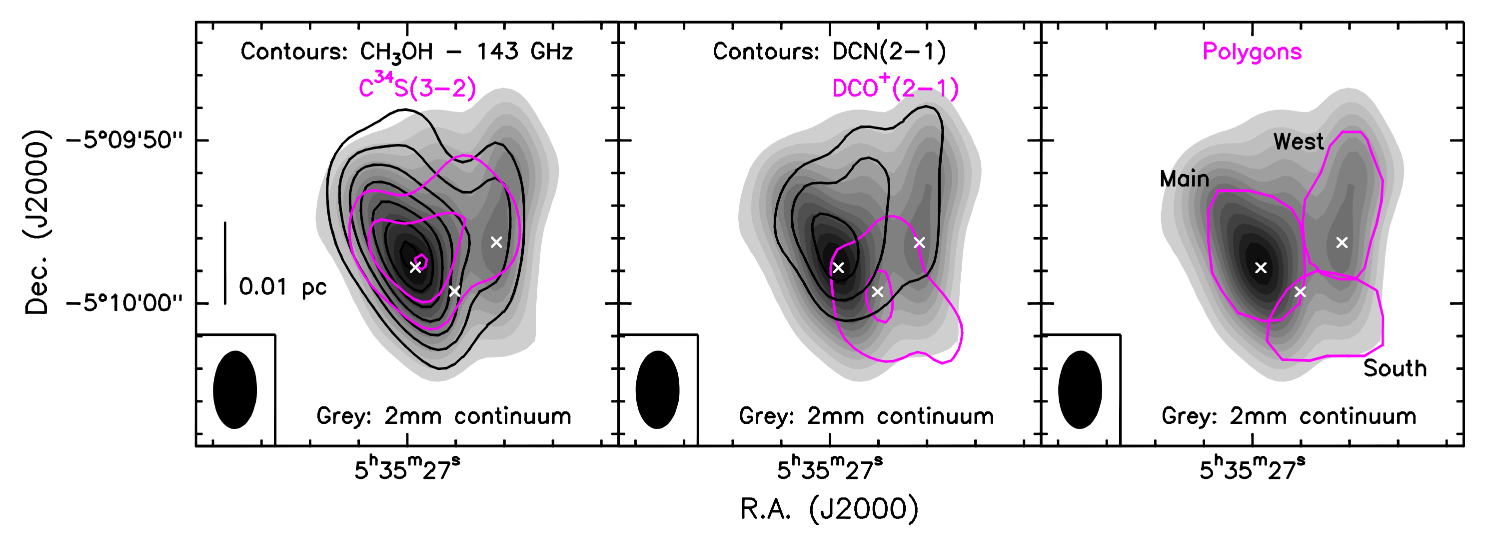

- Geometrical dilution factor:
  - free-streaming case → R^{-2}
  - diffusion with $R_{\rm diff} \gg R$ → R^{-1} (Aharonian 2004)

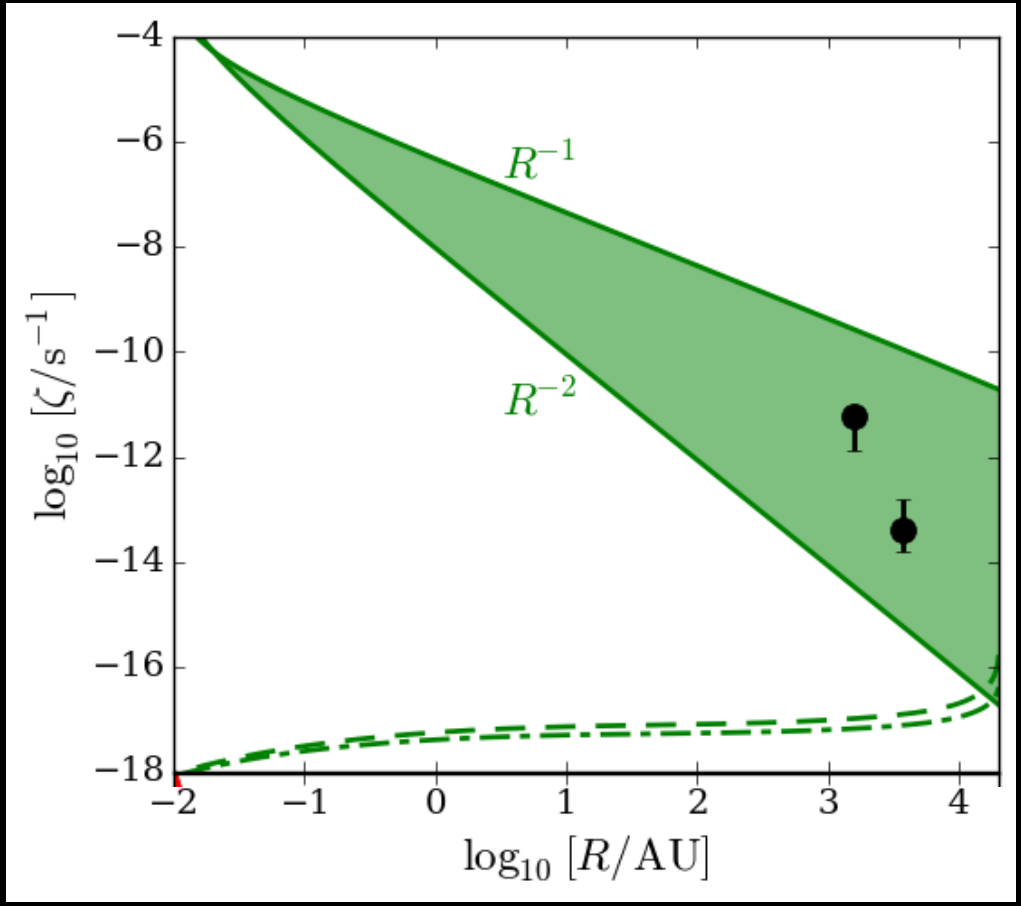

POSTER #13
Ana López Sepulcre

→ The propagation mechanism is probably neither purely diffusive nor free streaming.

Application of the modelling: comparison with available observations

Local CRs could be responsible for the formation of short-lived radionuclei (^{10}Be) contained in calcium-aluminium-inclusions of carbonaceous meteorites.

$[^{10}\mathrm{Be}]_{\mathrm{meteorites}} \gg [^{10}\mathrm{Be}]_{\mathrm{ISM}}$.

Hypothesis: *spallation reactions* during the earliest phases of the protosolar nebula.

Fluence per unit time: $$\mathcal{F}_t(E_{\rm min}) = 2\pi \int_{E_{\rm min}}^{E_{\rm max}} j(E)\mathrm{d}E$$

$E_{\rm min} \simeq 50$ MeV: energy threshold for $p + ^{16}\mathrm{O} \rightarrow ^{10}\mathrm{Be} + \ldots$

$\mathcal{F}_t = 2\times10^{17}$ protons cm^{-2} yr^{-1} (purely diffusive case)
$\mathcal{F}_t = 8\times10^{18}$ protons cm^{-2} yr^{-1} (free-streaming case)

An irradiation of few tens of years can explain the values of the fluence derived by Gounelle+ (2013) equal to 10^{19}-10^{20} protons cm^{-2}.

In high-mass YSOs it is even easier to accelerate CRs!

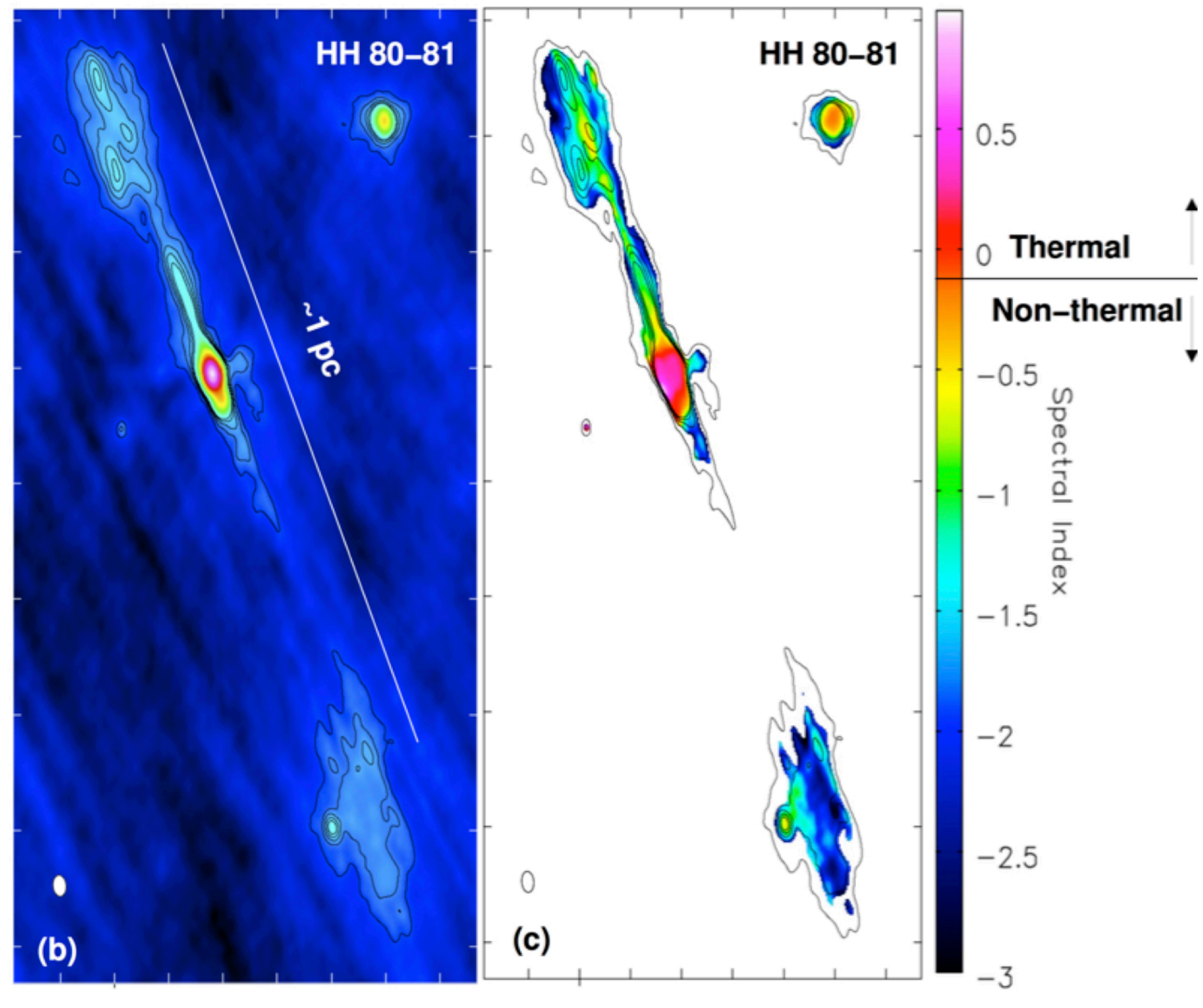

Carrasco-González+ (2013)

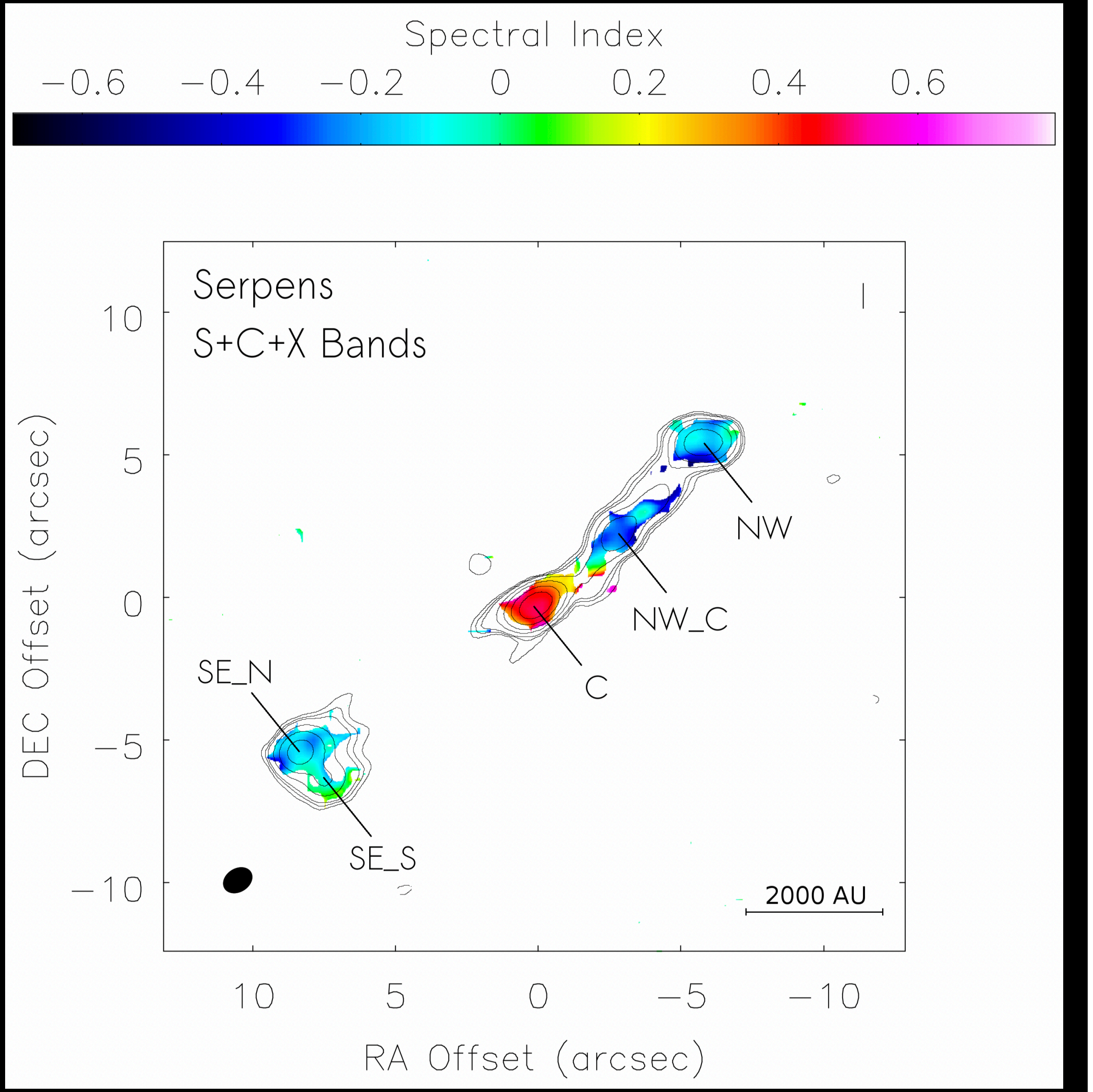

Rodríguez-Kamenetzky+ (2015)

In high-mass YSOs it is even easier to accelerate CRs!

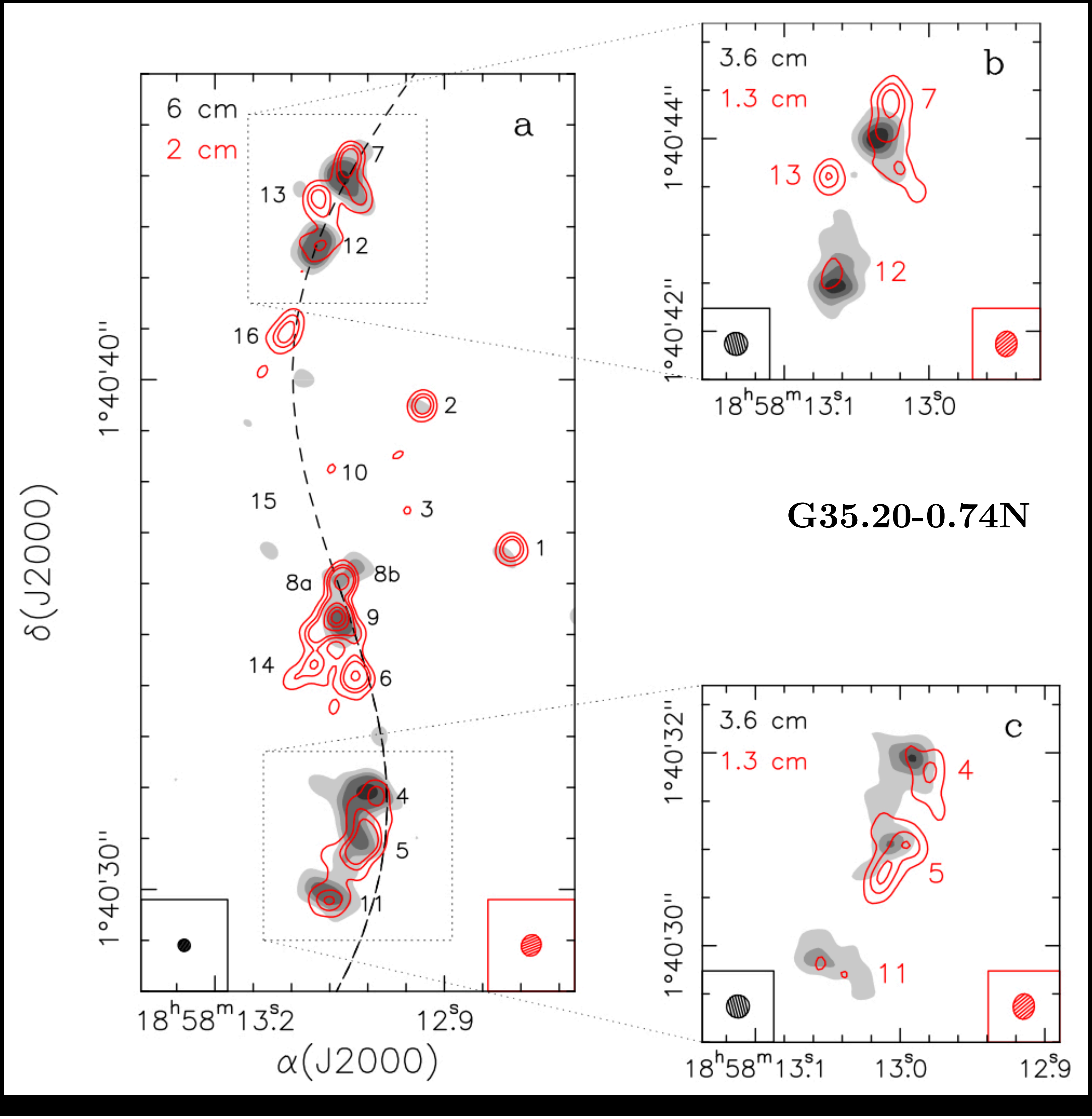

G35.20-0.74N

Beltrán+ (2016)

Other acceleration and ionisation mechanisms

Shear acceleration

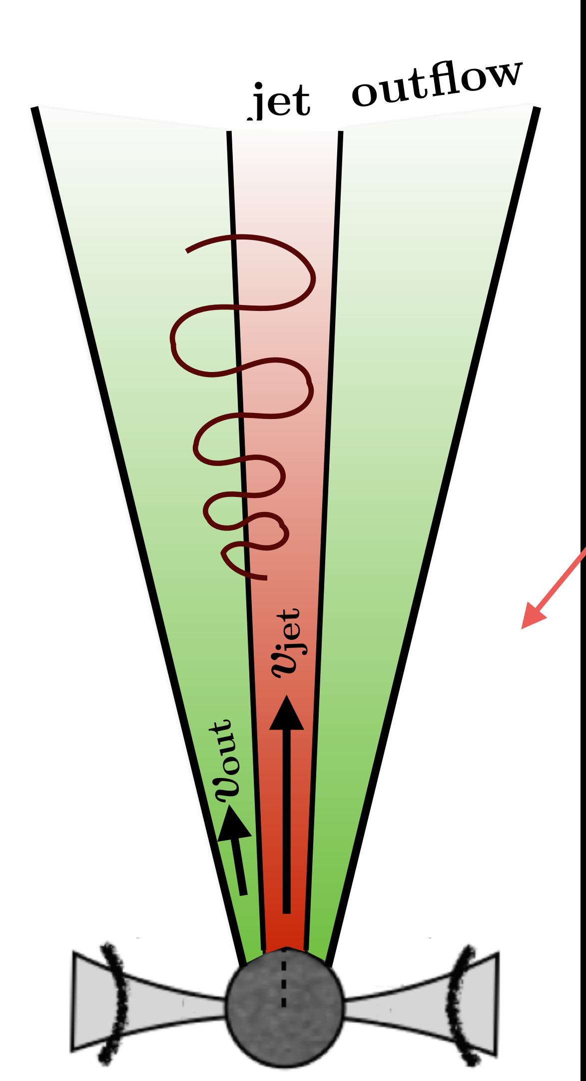

Higher geometrical efficiency with respect to shock acceleration.

Magnetic reconnection

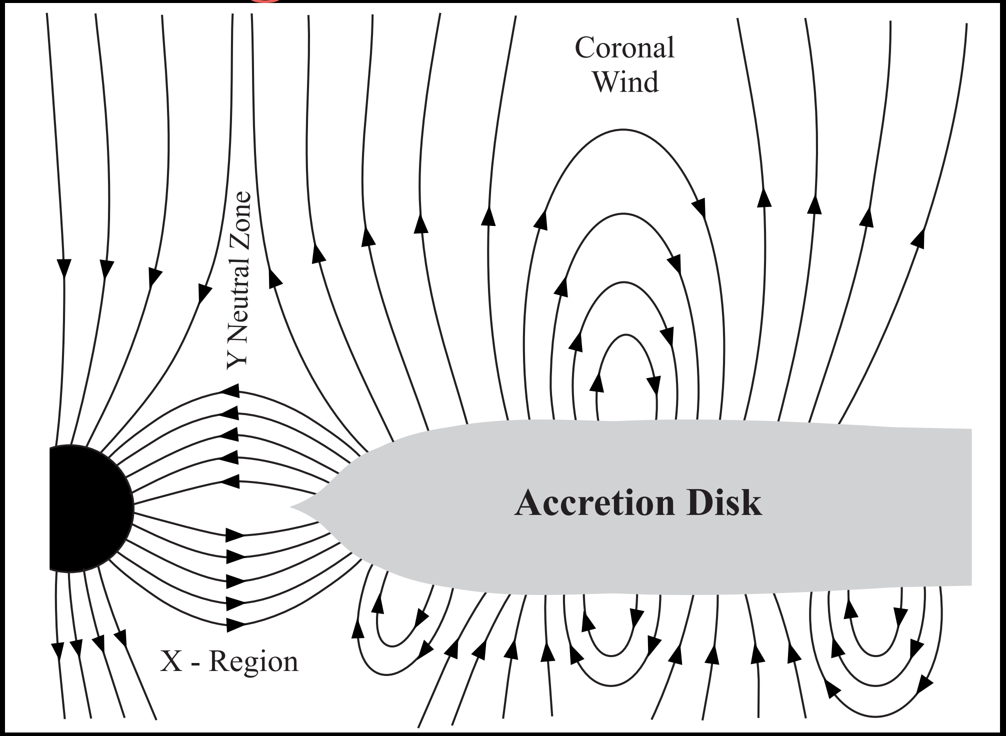

de Gouveia Dal Pino & Lazarian (2005)

X-ray ionisation

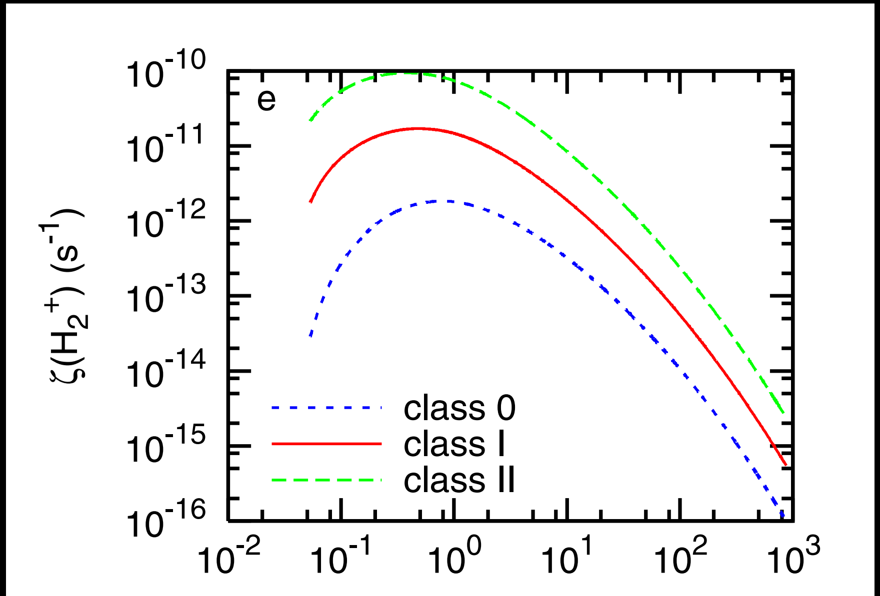

Panoglou+ (2015)

Conclusions and Perspectives

- We identified a new mechanism to accelerate CRs in protostellar shocks.
- A number of observations can be explained by our modelling: synchrotron emission in DG Tau, ionisation rate in L1157-B1 and OMC-2 FIR 4.
- High-resolution observations (e.g. with ALMA and NOEMA) will help to have better constraints, with a special consideration for the magnetic field configuration. We need more statistics (including high-mass protostars).
- Outcomes on: the formation of meteoric ^{10}Be;
  the creation of COMs on dust grains + release in the gas phase;
  the extension of dead zone in discs.